AD-A112 523 MASSACHUSETTS INST OF TECH LEXINGTON LINCOLN LAB F/G 22/2
TECHNOLOGY ASSESSMENT: OPTICAL COMMUNICATIONS, SIGNAL PROCESSOR--ETC(U)
JAN 82 L J RICARDI, D M BOROSON, V W CHAN F19628-80-C-0002
UNCLASSIFIED ESD-TR-81-333 NL

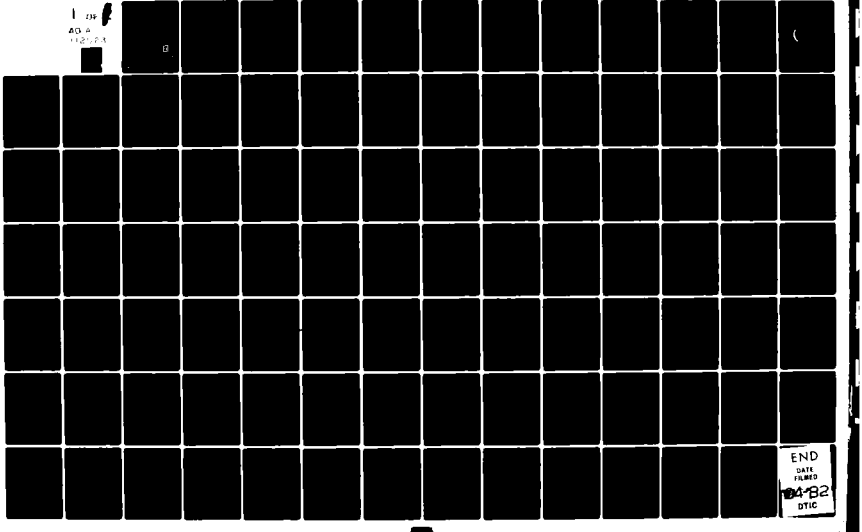

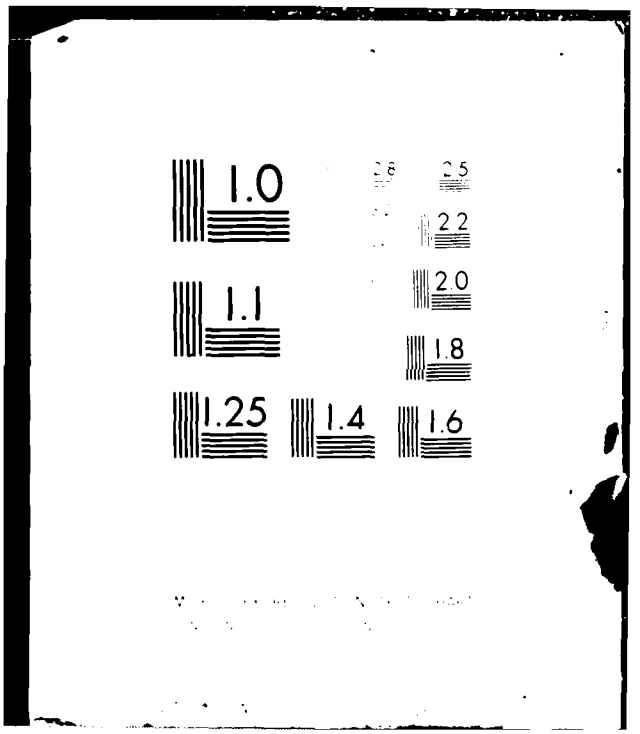
1.0
2.8
2.5
2.2
1.1
2.0
1.8
1.25
1.4
1.6

ESD-TR-81-305

(12)

Project Report

DCA-11 ✓

Technology Assessment: Optical Communications, Signal Processors, and Radiation Effects

7 January 1982

Prepared for the Department of the Air Force
and the Defense Communications Agency
under Electronic Systems Division Contract F19628-80-C-0002 by

Lincoln Laboratory

MASSACHUSETTS INSTITUTE OF TECHNOLOGY

Lexington, Massachusetts

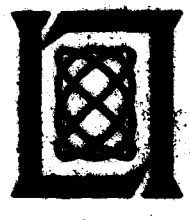

Approved for public release; distribution unlimited.

DTIC
ELECTE
MAR 25 1982
S H D

FILE COPY

82 03 25 002

The work reported in this document was performed at Lincoln Laboratory, a center for research operated by Massachusetts Institute of Technology. This work was sponsored in part by the Department of the Air Force and in part by the Military Satellite Communications Systems Office of the Defense Communications Agency under Air Force Contract F19628-80-C-0002.

This report may be reproduced to satisfy needs of U.S. Government agencies.

The views and conclusions contained in this document are those of the contractor and should not be interpreted as necessarily representing the official policies, either expressed or implied, of the United States Government.

The Public Affairs Office has reviewed this report, and it is releasable to the National Technical Information Service, where it will be available to the general public, including foreign nationals.

This technical report has been reviewed and is approved for publication.

FOR THE COMMANDER

Raymond L. Loiselle

Raymond L. Loiselle, Lt.Col., USAF
Chief, ESD Lincoln Laboratory Project Office

(12)

MASSACHUSETTS INSTITUTE OF TECHNOLOGY

LINCOLN LABORATORY

TECHNOLOGY ASSESSMENT: OPTICAL COMMUNICATIONS, SIGNAL PROCESSORS, AND RADIATION EFFECTS

L.J. RICARDI

Editor

D.M. BOROSON
V.W.S. CHAN
B.H. HUTCHINSON
E.G. WALTHER
J.P. WOODS
S.L. ZOLNAY

Division 6

PROJECT REPORT DCA-11

7 JANUARY 1982

Approved for public release; distribution unlimited.

LEXINGTON MASSACHUSETTS

Abstract

Military satellite communication system architects are often constrained by the performance capability of technology limited devices. Consequently, it is important to continually assess that technology essential to the support of future MILSATCOM systems. This project report and those published previously[1,2,3] summarize study efforts that developed strawman MILSATCOM systems which satisfy projected user requirements. The technology requisite to deployment of these SATCOM systems was carefully evaluated, and required improvements were described and/or defined. Previously[1,2,3], the study was limited to RF devices or related phenomena. This report considers optical communication systems, on-board signal demodulators, and radiation effects. An update on the traveling-wave tube technology is presented because of its extreme importance to the development of affordable MILSATCOM terminals.

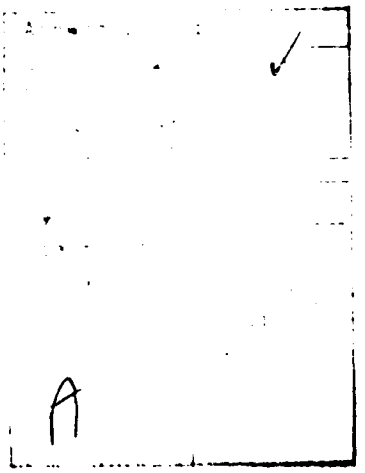

CONTENTS

CONTENTS (cont'd)

ILLUSTRATIONS

TABLES

I. INTRODUCTION

The Military Satellite Communications (MILSATCOM) Systems Office (MSO) of the Defense Communications Agency (DCA) must continually review that technology requisite to the development of MILSATCOM architecture in order to fully utilize advanced technical achievements, ideas, etc., in advancing the capability and improving the performance of future MILSATCOM systems. Lincoln Laboratory aids the MSO in this function by surveying and assessing the associated technology. In addition to using the results of these studies to guide the architectural decisions, Department of Defense (DoD) sponsored research and development support could be guided toward those areas where it was needed and could prove most beneficial.

In most recent years, the survey was preceded by examining the MILSATCOM requirements and synthesizing an EHF strawman MILSATCOM system that could meet these requirements. The frequencies of interest were chosen in the EHF band in accordance with direction from Congress, potential anti-jam (AJ) improvements of EHF over lower frequency systems. The survey was needed because a great deal of general knowledge about EHF devices, and propagation of electromagnetic waves was lacking and yet necessary to adequately assess the potential performance characteristics of EHF systems. A strawman system was synthesized in order to identify those components that must be developed, what performance characteristics they must have, and when they would be needed. Analysis of the strawman system surfaced those phenomena, such as attenuation due to rain, that needed investigation or further study. Similar efforts initiated a fresh look at electronic and physical threats and the

development of several "typical" scenarios that provide a "common proving ground" for all MILSATCOM systems regardless of operating frequency. The results of these efforts were reported extensively; the Lincoln Laboratory effort carried out under contract with the DCA/MSO was reported in three documents.[1,2,3]

These Lincoln Laboratory Project Reports received widespread distribution within the DoD and were used to guide the services in preparation of the Research and Development Program Object Memorandum (R&D/POM). Due to contemporary issues, they were focussed on RF components and phenomena. These documents and the effort they report do not bring this effort to an end, but it was felt at the beginning of FY'81, that the emphasis of the survey should be shifted to include MILSATCOM systems using optical communication and on-board signal processors. Consequently, this report provides an initial assessment of an optical communications system, and signal processors with special attention to radiation effects and a brief update on traveling wave tubes.

II. OPTICAL COMMUNICATIONS

A. Introduction

Optical satellite communication (SATCOM) systems can be an attractive alternative to millimeter-wave military SATCOM systems, particularly when the data rate required is high. Figure 1 depicts some examples of optical SATCOM systems. Small size antenna aperture is one main advantage of optical over millimeter-wave systems. Figure 2 compares the antenna aperture size required for 60 GHz and optical crosslinks as a function of data rate. These results are for point system designs based on state-of-the-art transmitter and receiver technologies. It is evident that for high data rates (> 10 Mbps), an optical system becomes the logical choice if minimum antenna aperture size is an important characteristic. Figure 3 compares the subsystem weight required by a 60 GHz and an optical communication crosslink. A somewhat smaller and less significant preference for optical communications is indicated if minimum weight is necessary and the data rate exceeds 10^7 bps. System analysis at the optical frequencies often differs significantly from that at lower frequencies due to the vastly different technologies of sources, modulators, and receivers and also due to the important role that nonclassical (quantum) noise plays in determining system performance. In this section, important optical communication system architectures and critical system and technology issues that affect system designs will be examined. Examples will be presented using current state-of-the-art tecnology. An assessment will follow pointing out those areas where development is required.

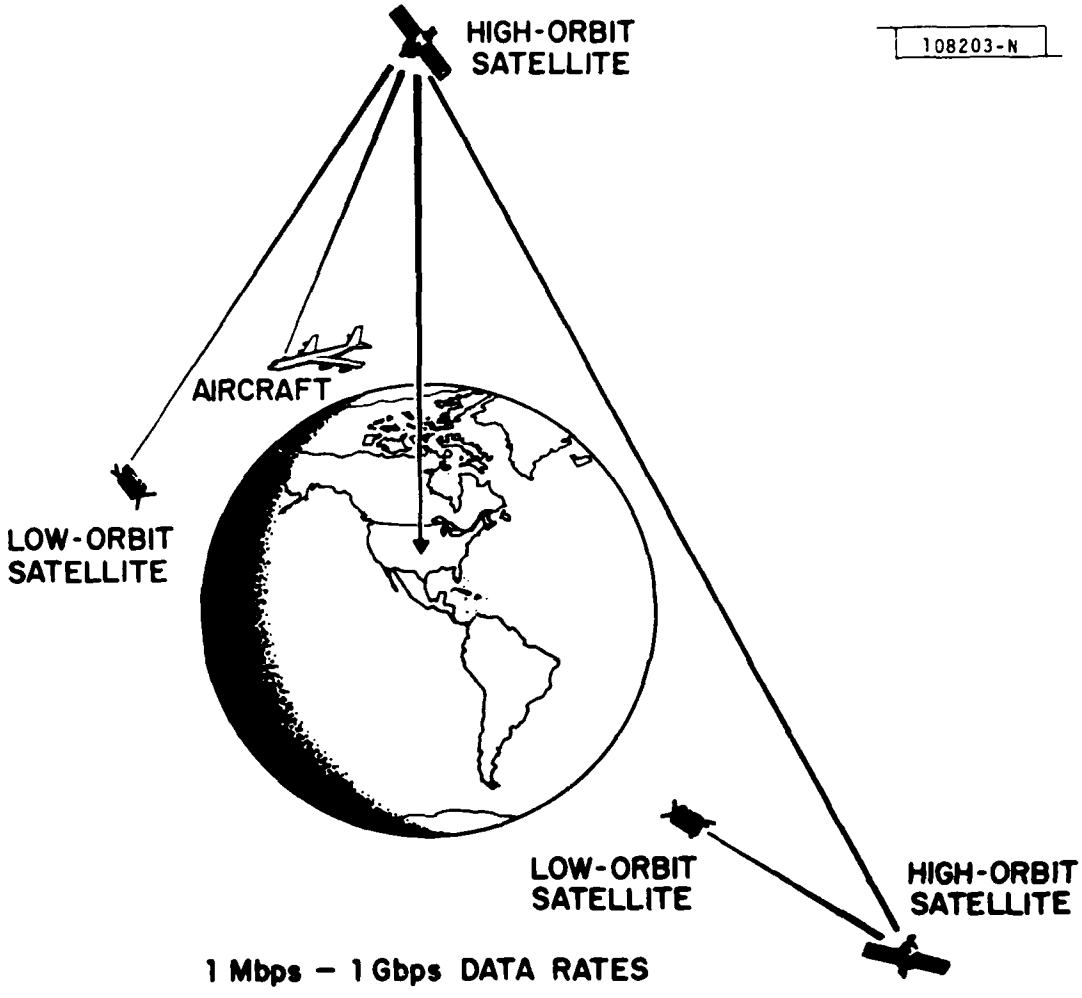

Fig. 1. Optical communication applications in space.

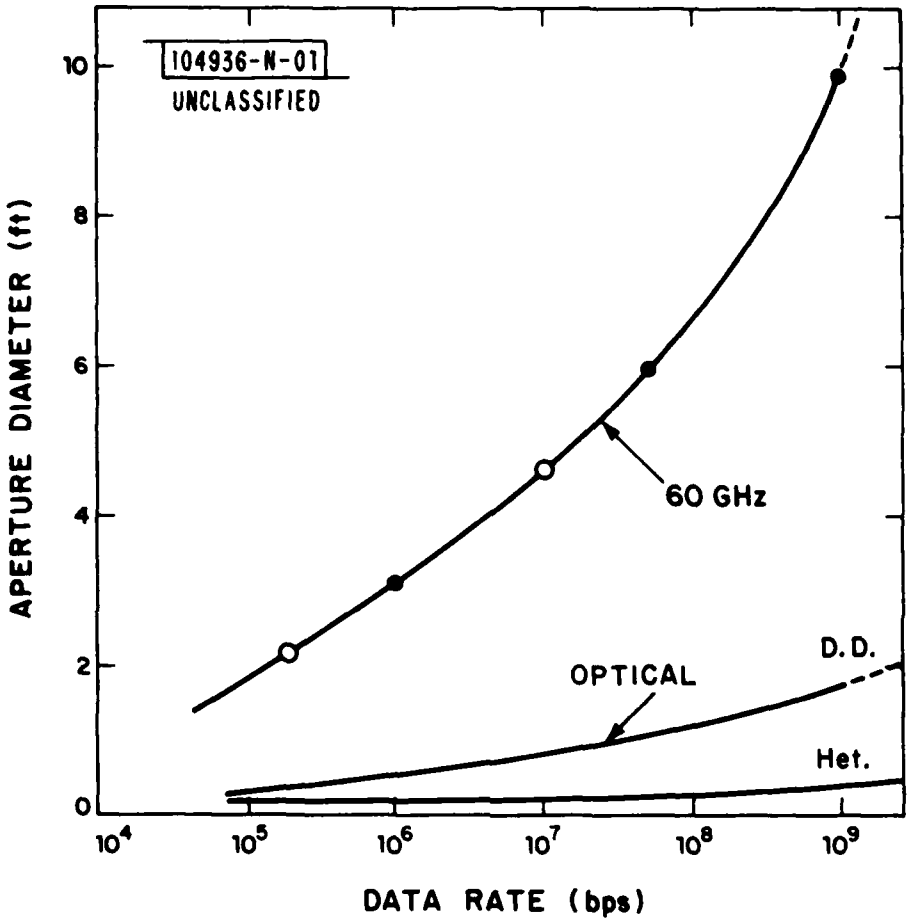

Fig. 2. Crosslink aperture diameter.

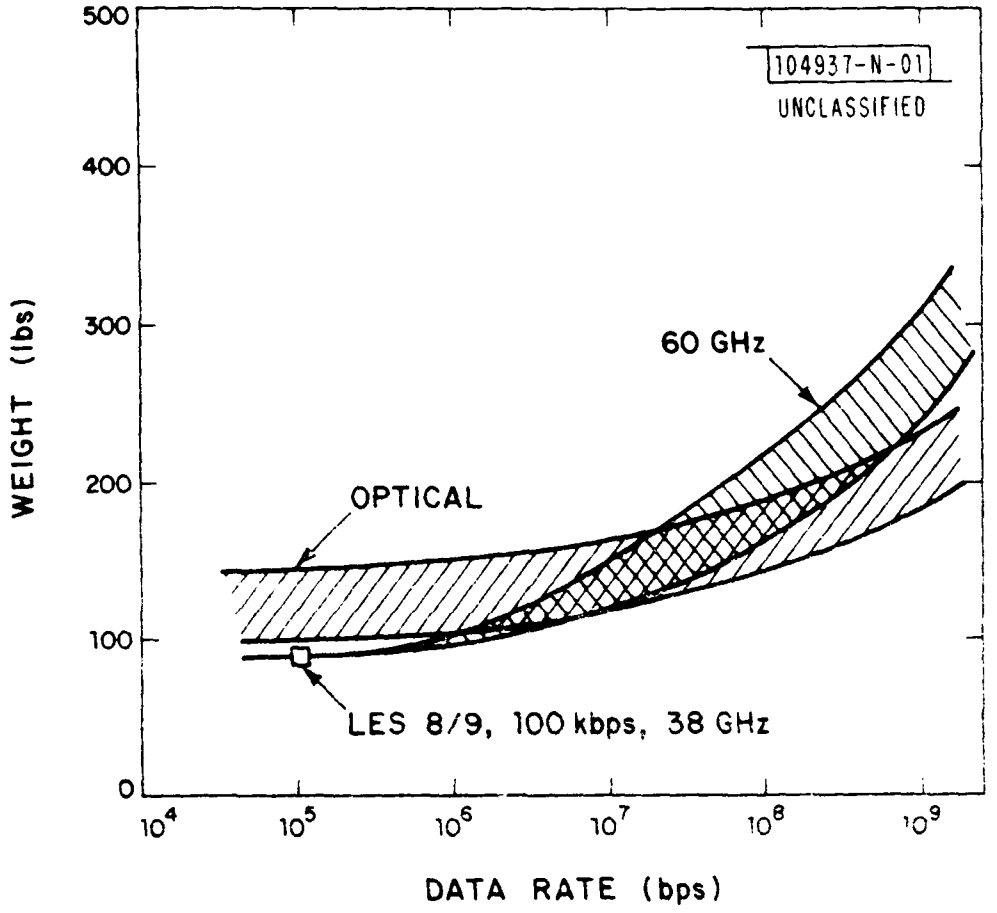

Fig. 3. Crosslink subsystem weight.

B. General Mission Requirements and Constraints

The class of optical channels encountered in space communications includes the satellite-to-satellite channel, the ground/aircraft-to-satellite and satellite-to-ground/aircraft channel (see Figure 1).* The data rate requirements may vary from 1 Mbps to 1 Gbps and can sometimes determine the associated system architecture to a considerable extent. Atmospheric turbulence, aircraft boundary layer effects, weather and ocean effects are some of the undesirable channel characteristics that must be considered. Still other factors (not unique to optical SATCOM systems) that need to be considered include link distance, relative velocity, point ahead angle, angular tracking rate, doppler shift, background radiation and satellite platform stability. All the ramifications of the channel characteristics and application parameters will not be discussed in this report, except to be mentioned in passing that all these factors should be considered when choosing any system architecture.

C. Desirable System Characteristics

The following is a list of desirable characteristics, not necessarily absolute requirements, for an optical point-to-point SATCOM system.

1. Small antenna aperture size ($\leq$ 10 cm) -- this characteristic is particularly desirable when there are multiple transmitters or receivers on a single platform such as the case of a satellite relay node where spacecraft real estate is precious.

*Optical links for satellite-to-underwater receiver operating at ~ 1 bps have been proposed; this report does not address this application.

2. Modest weight (100-200 lbs) and power (100-200 W) — this and the previous characteristic are especially desirable when the optical COMSAT package is a secondary payload on a satellite.
3. Common technology and system architecture for a wide range of data rates - this is desirable to minimize cost of and permit interoperability among future systems.
4. Easy multiplexing/demultiplexing and switching
5. Operation with Sun in receiver field of view
6. Operational life greater than seven years
7. Reliable source of supply of essential components

D. Optical Communication System Architectures

There are two basic classes of optical receivers; their salient difference is centered on the detection method which can be either coherent (heterodyne or homodyne detection) or incoherent (direct detection). Usually the application will determine which one of these two basic receiver concepts is more appropriate. System requirements and channel effects will also influence the system architecture and choice of its parameters.

In an incoherent detection system (Fig. 4), the received optical energy is detected by means of a photodetector that usually provides signal gain (e.g., a photo-multiplier tube (PMT) or an avalanche photo-detector (APD)). Some front-end gain at, and preferably integrated with, the detector is required because of the low signal power received (typically around 100 photons per information bit). Since the frequency and phase of

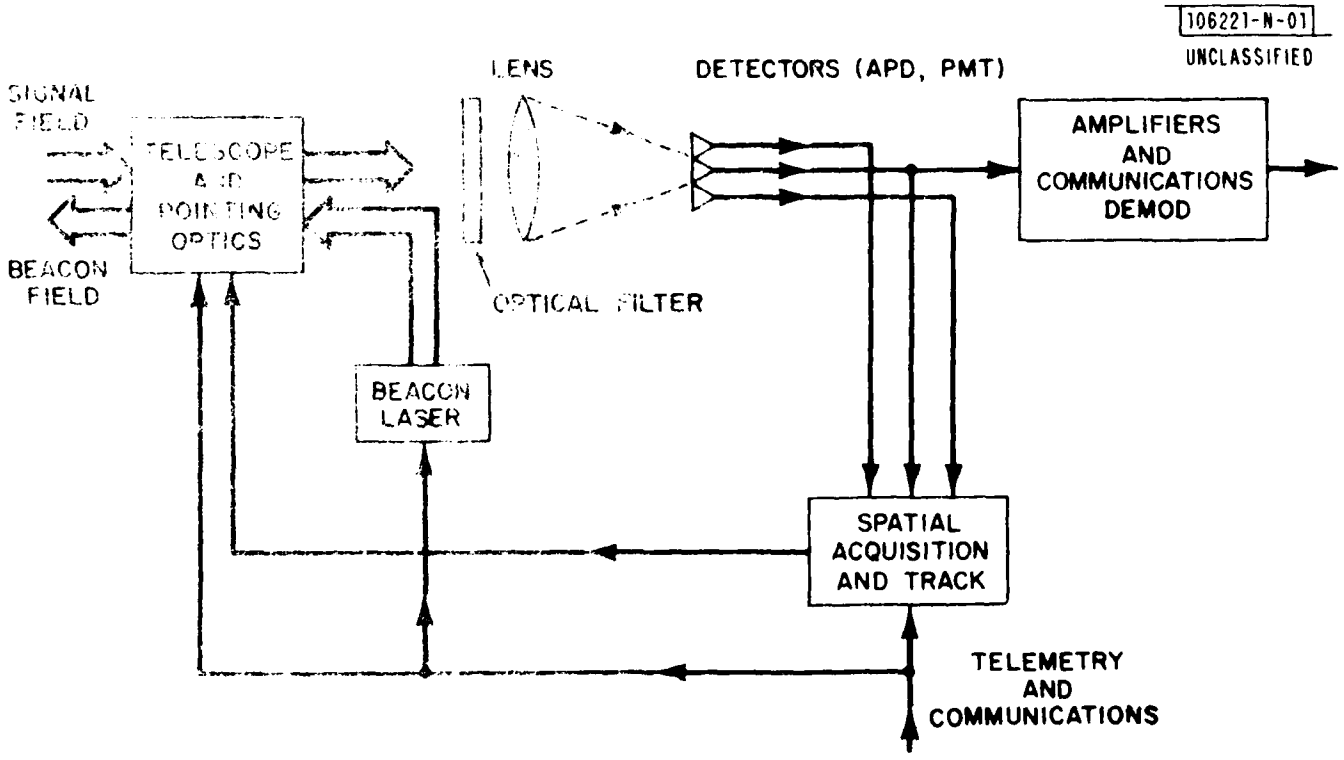

Fig. 4. Direct detection receiver.

the optical field are irretrievably lost in the energy detection process, these systems are limited to various types of intensity or polarization modulation.

Multimode direct detection can usually be assumed. Consequently, the detector either observes many spatial modes (i.e., a large field of view) and/or many temporal modes exist. Observation over a large number of temporal modes occurs when the product of optical detector bandwidth, B_c, and the average interval between photon arrivals, t_a, is much larger than unity (i.e., $B_c t_a \gg 1$). Since $t_c = 1/B_c$ is the coherence time of the arriving photons, the above condition becomes $t_a \gg t_c$, which is called the "Weak Photon Coherence Assumption". Under this assumption, the stochastic photon arrival rate parameter can be replaced by its expected value, and the resulting detection process for coherent light in background noise becomes Poisson distributed. Given that one chooses binary signaling, on-off-keying is the optimum signal set. However, the degree to which this signal set is optimum depends on the choice of detection threshold based on the precise knowledge of the signal level at the receiver, which is typically not the case. On the other hand, pulse position modulation (PPM), which is usually preferred, is only 3 dB poorer in performance than on-off-keying, for binary signaling, and PPM becomes the optimum signal set as the symbol size increases. Let us next develop a performance measure for PPM.

For equiprobable inputs, the maximum-likelihood decision receiver minimizes output symbol error probability. The sufficient statistic is (n_j) $j=1,\ldots, N$, where n_j is the photon count in the j^{th} time slot. If the message m_i was sent, the expected number of photons in the j^{th} slot is λ_j for $J \neq I$

and $\lambda_s + \lambda_n$ for j=l, where λ_n is the average background noise count per time slot and λ_s is the average signal count per channel symbol. The optimum receiver picks the message m_k corresponding to the slot which yielded the maximum count.

The Chernoff Bound that gives the tightest exponential bound to the channel symbol error probability is

$$\Pr[\epsilon] \leq (M-1) \exp\{-(\sqrt{\lambda_s + \lambda_n} - \sqrt{\lambda_n})^2\}$$

$$= (M-1) \exp\{-\lambda_s E(\mu)\} \qquad (1)$$

$$\lambda_n = \eta \lambda^2 \Delta\lambda N_\lambda T/hc$$

is the average number of background counts, with η being the detector quantum efficiency, T the duration of a slot, $\Delta\lambda$ the bandwidth of the optical filter in wavelength units, and N_λ the background light spectral irradiance. Define

$$\mu = \lambda_s/\lambda_n \quad , \qquad (2)$$

the signal-to-background ratio, and,

$$E(\mu) = (\sqrt{1 + 1/\mu} - \sqrt{1/\mu})^2 \quad , \qquad (3)$$

is a bound parameter having the following properties:

1. as $\mu \to \infty$, $E(\mu) \to 1$ and quantum limited performance is attained.
2. as $\mu \to 0$, $E(\mu) \to \mu/4$ and the performance is background limited.

Note that transition between these two regions occurs around $\mu = 4$.

Since the only background noise filtering in an incoherent system is provided by the optical filter which typically has a wide pass-band, communication performance can be background-noise-limited, particularly when the Sun is in the receiver field of view, or when the field of view is wider than diffraction-limited (e.g., in a direct detection receiver, to help spatial acquisition and tracking, the field of view can be increased by choosing a detector area larger than the diffraction-limited Airy Disc area). Background-limited performance can be avoided by choosing the optical filter bandwidth such that $4\lambda_n < \lambda_s$. Unfortunately, the bandwidth of the optical filter cannot be chosen arbitrarily small because the receiver may not be tuned to the transmitter frequency with a sufficient degree of accuracy. For example, if a semiconductor laser is used, the filter bandwidth most likely will have to be a few angstroms, unless a frequency-reference-and-control (FRC) system is employed to "tune" the receiver.

The system can also be detector-noise-limited if the quantum efficiency of the photon detector is not unity or the gain of the detector is noisy, as in an APD[4]. Note, for λ_n=1 and binary signaling, an average of λ_s=21 detected signal photons per bit is required to obtain a 10^{-6} BER (bit error rate). The required amount of received signal photons per bit can increase substantially due to APD noise (13-16 dB for Si APD's operating at .85 μm and ~ 21 dB for Ge or GaInAsP APD's operating at 1.3 μm).

In a coherent system (Fig. 5), an optical local oscillator field is added to the received optical field such that the sum of these fields illuminates a photo-detector which is followed by appropriate processing at an intermediate frequency (heterodyne detection) or at baseband (homodyne detection).

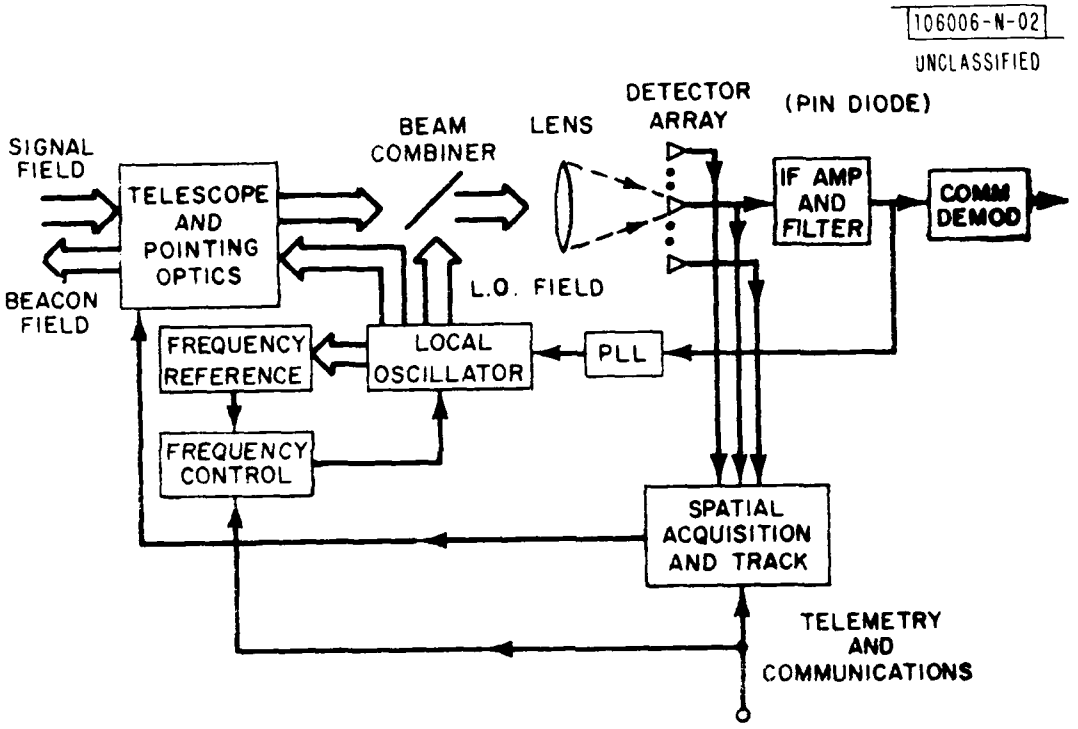

Fig. 5. Heterodyne receiver.

The front-end of a coherent receiver acts as a linear amplifier and converts the received optical field to an electrical output, and a detector that can provide signal gain is not necessary. As the local oscillator power is increased, the system becomes quantum-noise-limited. The output noise process can be modeled as white gaussian with power spectral density $N_0/2 = h\nu/2\eta$ for a heterodyne and $h\nu/4\eta$ for a homodyne system, where h is Planck's Constant, ν is the frequency of the optical field, and η is the quantum efficiency of the photodetector. Communication theory for signals in additive white gaussian noise is well understood.[5] Given that one chooses binary signaling, binary antipodal signaling (e.g., BPSK Phase Shift Keying) is the optimum signal set. The channel bit error probability of an uncoded channel is given by

$$Pr(\varepsilon) = Q(\sqrt{2E_s/N_0}) \leq \frac{1}{2}\exp(-E_s/N_0) \qquad (4)$$

where Q is the gaussian error function and E_s is the received signal-energy-per-bit in Joules.

For 10^{-6} channel-bit-error probability, $(E_s/N_0) = 13.1$ (11.4 dB). At a 1-μm wavelength, this means that the received power required at the detector for a 1-bps data rate must be at least 2.6×10^{-13} W. The use of a larger symbol size (such as M-ary FSK with large M) can lower the (E_s/N_0) requirement to approach the information-theoretical limit of $\ln 2 = 0.693$ (-1.6 dB). This represents a substantial improvement over small M; however, the use of a larger symbol size typically requires improved frequency-tracking requirements. Since a heterodyne receiver requires phase-tracking or

frequency tracking of the received optical signal field, a feedback tracking loop is required. It need not operate at optical frequencies (see Chapter 4, Fig. 3) in practice, it could be a carrier optical/IF loop. For some applications, the relative motion of the transmitter and receiver may be so severe that phase tracking may be impossible. In that case, phase modulation of the optical field cannot be properly demodulated and incoherent FSK becomes the logical modulation. The performance of an incoherent FSK signaling scheme operating at error rates $< 10^{-6}$ is about 3 dB worse than coherent BPSK. Using a larger symbol size can improve performance.

In addition to an optical filter for background noise rejection, a heterodyne receiver also has an IF filter that performs additional filtering of noise processes. With this, a heterodyne receiver can be made essentially blind to the interference of sunlight even if the Sun is within the receiver field of view.

Since the optical signal field must mix with the local oscillator field at the detector, a heterodyne receiver has a diffraction-limited field of view. To increase the receiver field of view for improved spatial tracking, an array of detectors with multispatial mode heterodyne detection using spherical wave mixing must be used (see Fig. 6). Unfortunately, this area of technology is not well established, particularly at the near IR and visible wavelengths.

To compare the coherent and incoherent systems in the same application, a link between two satellites in a synchronous orbit and separated by 22,000 miles will be considered. The device parameters chosen for this exercise are given in Tables I and II. They represent projected near-term state-of-the-art

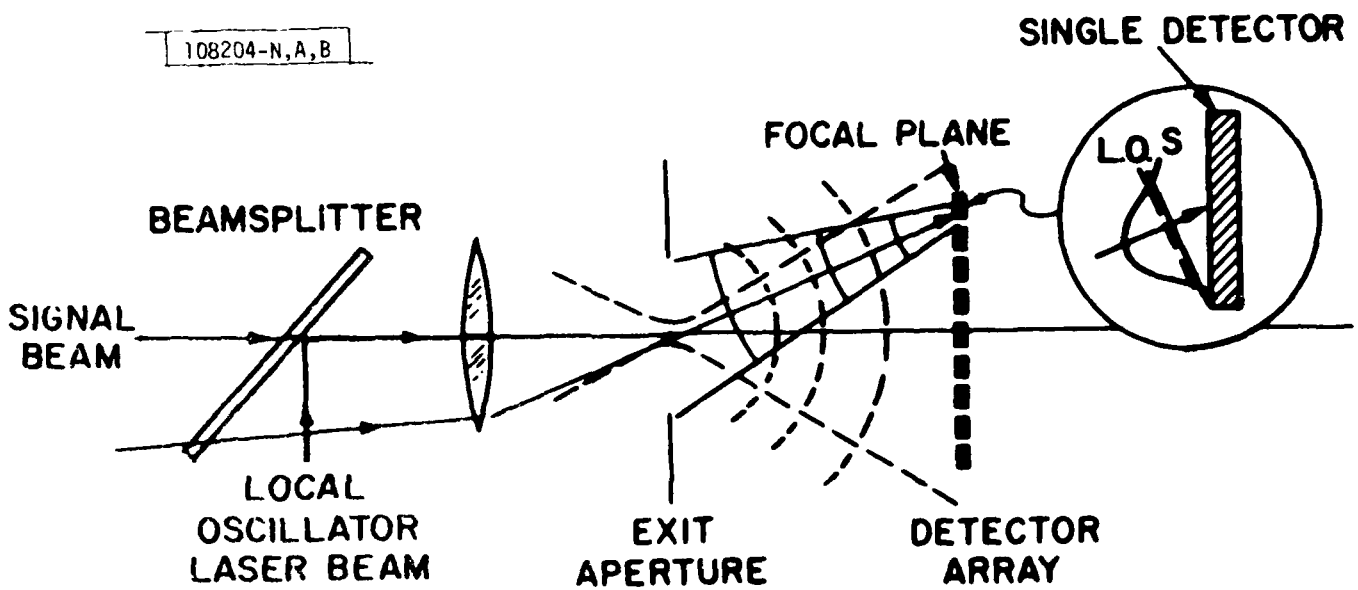

Fig. 6. Multimode heterodyne detection using spherical wave mixing.

TABLE I

SYSTEM PARAMETERS USED IN REFERENCE DIRECT DETECTION SYSTEM

- Binary PPM signaling
- 3 Å optical filter
- APD detectors(Si), Excess noise factor - 5, Q.E. - 90%
- 0.2 ns pulse width
- 5 dB optics loss
- 7 dB link margin
- 10 cm transmit/receive apertures
- 4 nW/bps required for 1 sync orbit path at 10^{-6} BER
- GaAlAs or Nd:YAG doubled

TABLE II

SYSTEM PARAMETERS USED IN REFERENCE HETERODYNE SYSTEM

- Binary PSK
- 10-30 Å optical filter
- PIN detectors (Si/Ge) Q.E. 90-100%
- GaAlAs or Nd:YAG in CW operation
- 3 dB optics loss
- 7 dB link margin
- 10 cm transmit/receive apertures
- 0.4nW/bps for 1 sync orbit path at 10^{-6} BER

technology. At present, incoherent systems possess [illegible] technology. The performance of these two "reference" systems [illegible] points corresponding to current state-of-the-art of incoherent technology are given in Fig. 7. Coherent systems are projected to require [illegible] [illegible] dB less transmitter power than incoherent systems [illegible] [illegible] However [illegible], coherent [illegible] technology is [illegible] not [illegible] be [illegible]

[illegible] potential [illegible] the following list of advantages and disadvantages of each system [illegible]

(i) Advantages of Incoherent (Direct Detection) Systems

(a) Receiver optics do not have to be diffraction-limited [illegible] bucket receiver can be used and spatial tracking is simple — ideal for wide field of view applications.

(b) Minimal requirements on laser temporal spectral purity. Frequency tracking is unnecessary.

(c) Current laser technology more mature.

(ii) Disadvantages of Incoherent (Direct Detection) Systems

(a) High peak power is required for background noise discrimination. This may present lifetime problems for lasers with peak power related damage mechanisms (e.g., semiconductor lasers).

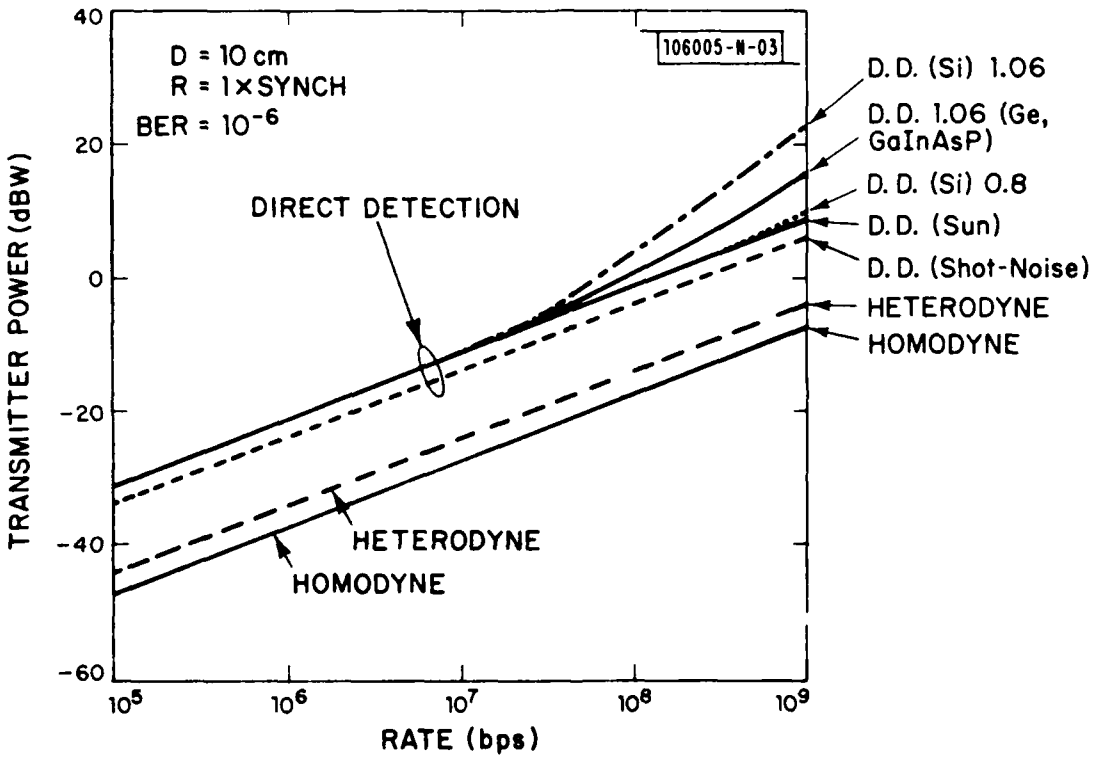

Fig. 7. Optical communication system performance.

(b) Communication performance can be background noise limited particularly when the Sun is in the receiver field of view.

(c) APD are noisy detectors, 10-15 dB loss in performance relative to a noiseless detector can be expected.

(d) Demodulation to bitstream at the receiver is required, making soft decision decoding for an end-to-end code difficult.

(iii) Advantages of Coherent Systems

(a) At least 10 dB better performance over incoherent systems at 1 μm (Fig. 7). Saving may be reflected in reduced weight and/or power.

(b) Solar blind and quantum limited performance.

(c) Easy multiplexing/demultiplexing -- demodulation to IF waveform is an attractive option for space relays.

(d) CW laser lifetime may be longer than high peak power pulsed lasers.

(e) Possibility of having commonality and interoperability for systems with different data rates.

(f) Possibility of 10 dB increase in system performance if large symbol size is used.

(v) Disadvantages of Coherent Systems

(a) Stable, single frequency laser required.

(b) Requires frequency acquisition and tracking.

[illegible]

[illegible]

[illegible]

[illegible]

[illegible]

[illegible] laser source at this time. Space qualifiable lasers [illegible] mode-locked and Q-switched Nd:YAG lasers are [illegible]. However, to make the Nd:YAG laser (or any other crystalline laser such as the Neodymium Pentaphosphate laser), a viable source for space applications, reliable and efficient pumps for the laser must be developed. Lamp-pumps are often used for crystalline lasers, but lamp lifetime is only around a few thousand hours. Moreover, these lasers are unattractive because their prime-to-laser output power conversion efficiency is typically < 0.1%. However, there are efforts ongoing to develop a GaAlAs laser pump for Nd:YAG type lasers with long lifetime and good power conversion efficiencies (~ 1%). This is a developing technology that will probably mature in a few years.

Development of detectors is another important technology area for incoherent optical communication systems. The avalanche photo-detector (APD) is the leading candidate; however, due to the fact that such devices have dark current, thermal noise and excess noise (multiplicative noise) associated with

the avalanche process, the ultimate performance of an incoherent system will unlikely be within 10 dB of the quantum limit at 0.9 μm using a silicon APD (within 18 dB for Germanium or GaInAsP APD operating at 1.3 μm). Fabrication of low noise detectors for incoherent receivers (e.g., photo-transistors, hybrid/integrated APD and matched trans-impedance amplifiers) is currently an active area of research and development.

The most critical development required for coherent systems is the stable and single frequency lasers required by the heterodyne receiver. These single frequency and stability requirements have ruled out heterodyne systems in the 1970's, with the exception of CO_2 systems. However, CO_2 system technology has not yet become space qualifiable. Around 10 W CW of CO_2 laser power is required for a 100 Mbps - 1 Gbps satellite communication system. Unfortunately, CO_2 lasers with this output power have a lifetime around 15,000 hours, far less the seven years desired for SATCOM systems. Moreover, for efficient operation (within 10 dB of the quantum limit) of the photo-mixing detector (HgCdTe) of a CO_2 heterodyne receiver, its operating temperature must be less than 130 K. The only proven spaceborne cryogenic system for long duration missions is a radiative cooler whose design has a significant impact on spacecraft configuration. A suitably small, low-power consuming, closed-cycle cooler has to be developed to make CO_2 systems a candidate for long durations space applications.

Crystalline lasers (such as the Nd:YAG laser) and semiconductor lasers (such as GaAlAs) also have great potential for use in coherent communication optical space systems. Recent technologies have matured to the point where

single frequency Nd:YAG and GaAlAs lasers can be fabricated. It remains to be determined if the frequency stability of these lasers is good enough for heterodyne reception purposes.

The Nd:YAG laser requires a traveling-wave, circulating-cavity construction (Fig. 8) to achieve high efficiency, stable, single frequency operation. For most satellite applications, an efficient laser diode, or light emitting diode, pump must be used to increase the prime-to-optical power conversion efficiency to at least 1%.

GaAlAs lasers are much more efficient (~ 10%) than crystalline lasers. Recently, frequency stabilization of a single longitudinal mode GaAlAs laser has been demonstrated using an external reference and a feedback thermal electric cooling element mounted at the laser heat sink (Fig. 9). Line-widths less than 1 MHz have been achieved, and the laser seems to be appropriate for heterodyne applications.

One advantage of crystalline lasers over semiconductor lasers is that there is an upper limit on output power per device for a semiconductor laser (~ 200 mW/device in the case of GaAlAs) due to optical power density related damage mechanisms. No such limit is present for crystalline lasers operating at about 1 W output power. Nonetheless, the performance curves in Fig. 7 indicate that using a heterodyne system, a few hundred mW of laser power at around 1 μm wavelength is adequate for a 1 Gbps system. If more received signal power is required, the transmitting and receiving optics aperture dimensions can be increased. Alternately, in any case, research and development efforts are underway to coherently lock multiple semiconductor lasers in order to transcend this apparent power limit.

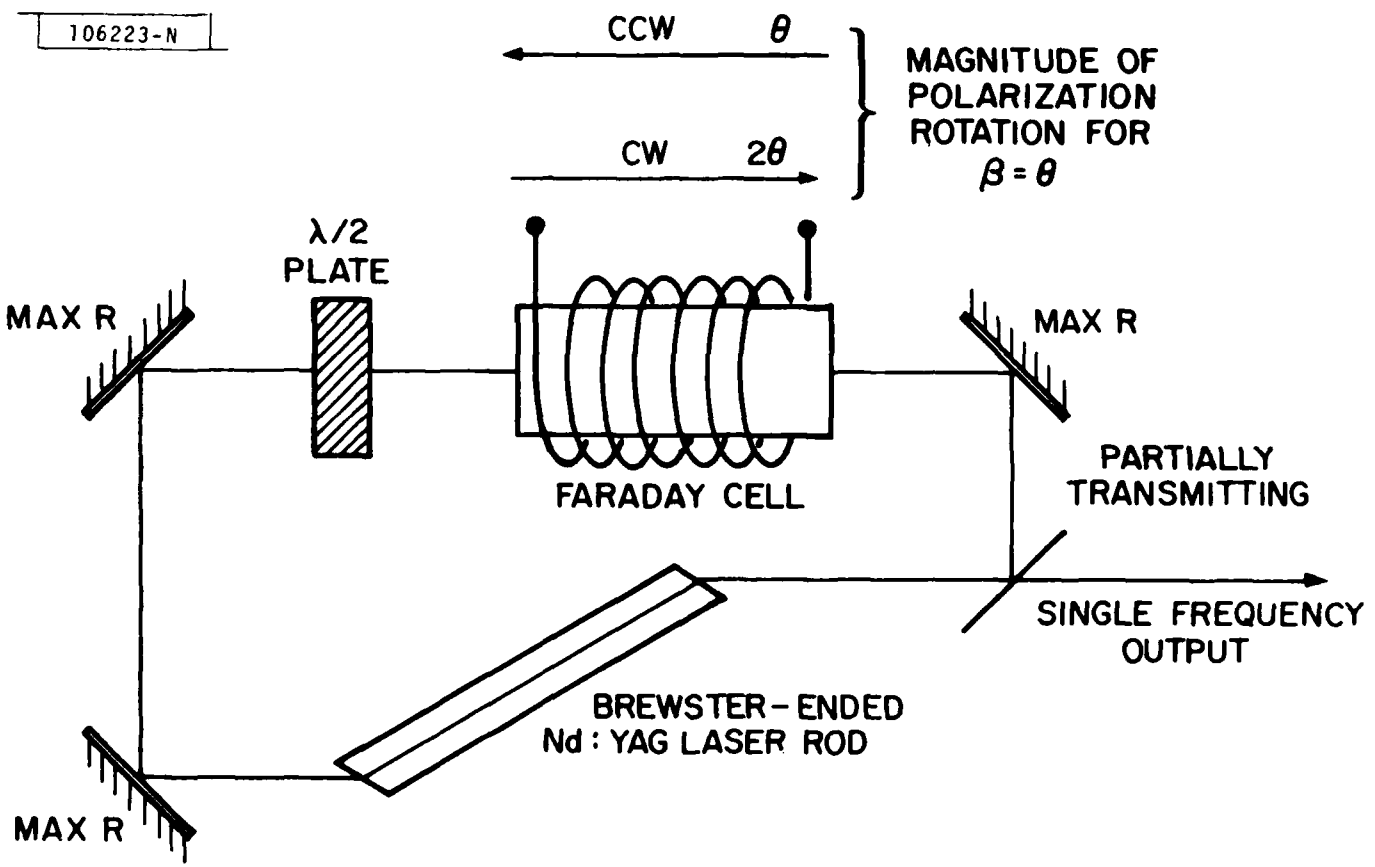

Fig. 8. Single-frequency traveling-wave Nd:YAG laser cavity configuration.

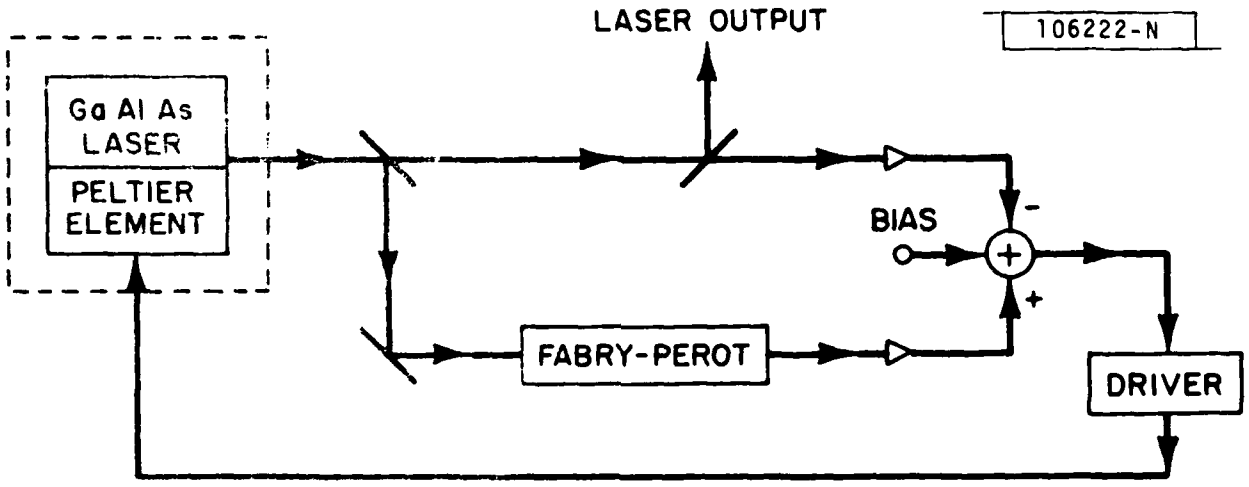

1 cm FABRY-PEROT

$\sigma_T \sim 10^{-3}$ K°

$\Delta_f < 1$ MHz

Fig. 9. Temperature controlled laser.

Detector technology appropriate for heterodyne systems at the near infrared and visible wavelengths seems mature (achieving ~ 90% quantum efficiency) at this time. Silicon photo-diodes should be used for the GaAlAs laser operating at 0.8 - 0.9 μm wavelength and Germanium or GaInAsP photo-diodes for wavelengths longer than 1 μm. There has been relatively little heterodyne experience at the 1 μm wavelength region, therefore, these detectors need to be characterized and studied in a heterodyne application.

F. Conclusions

System architectures and technologies for coherent and incoherent optical space communication systems have been discussed. At present, incoherent systems possess the more mature technology. However, it can be shown that with coherent systems, around 10 dB improvement in performance (and, therefore, reduced weight and power) is possible if suitably stable lasers are available to allow use of heterodyne or homodyne detection.

III. SPACECRAFT SIGNAL PROCESSOR TECHNOLOGY FOR MEDIUM-RATE POINT-TO-POINT COMMUNICATIONS SERVICE

A. Introduction

This section describes a design example to investigate the technology for spacecraft on-board signal processors for medium data rate point-to-point communications service. "Medium" is taken to mean user data rates of 20 to 200 kbps per terminal. This falls between typical per terminal mobile/tactical user data rate requirements of 0.1-10 kbps and wideband data requirements of 0.5 to 50 Mbps per terminal. The MCOS (Multi-Channel Objective System) for the GMF (Ground Mobile Forces) is a familiar example of such a medium-data-rate requirement; however, the spacecraft signal processing technology is not limited to or driven by that particular requirement. It is helpful to have some specific requirement in mind to help focus a technology investigation, and MCOS has played that role in this study.

An uplink demodulator with time acquisition and tracking capability is the key spacecraft processor development item for medium-rate service. The other required subsystems and components of a spacecraft signal processor are either the same as or a straightforward extension of those needed for service to mobile/tactical users. These other major components, developed as part of the test bed hardware effort for Lincoln Laboratory's Current System, include wideband fast frequency-hopping synthesizers, a downlink formatter or COP (Communications Output Processor), and a programmable controller to set up and control the other elements of the processor payload called the MARC, or Microcomputer Adaptive-Routing Controller (see Fig. 10). For medium-rate MCOS-type service, the frequency-hopping synthesizers are the same. The MARC

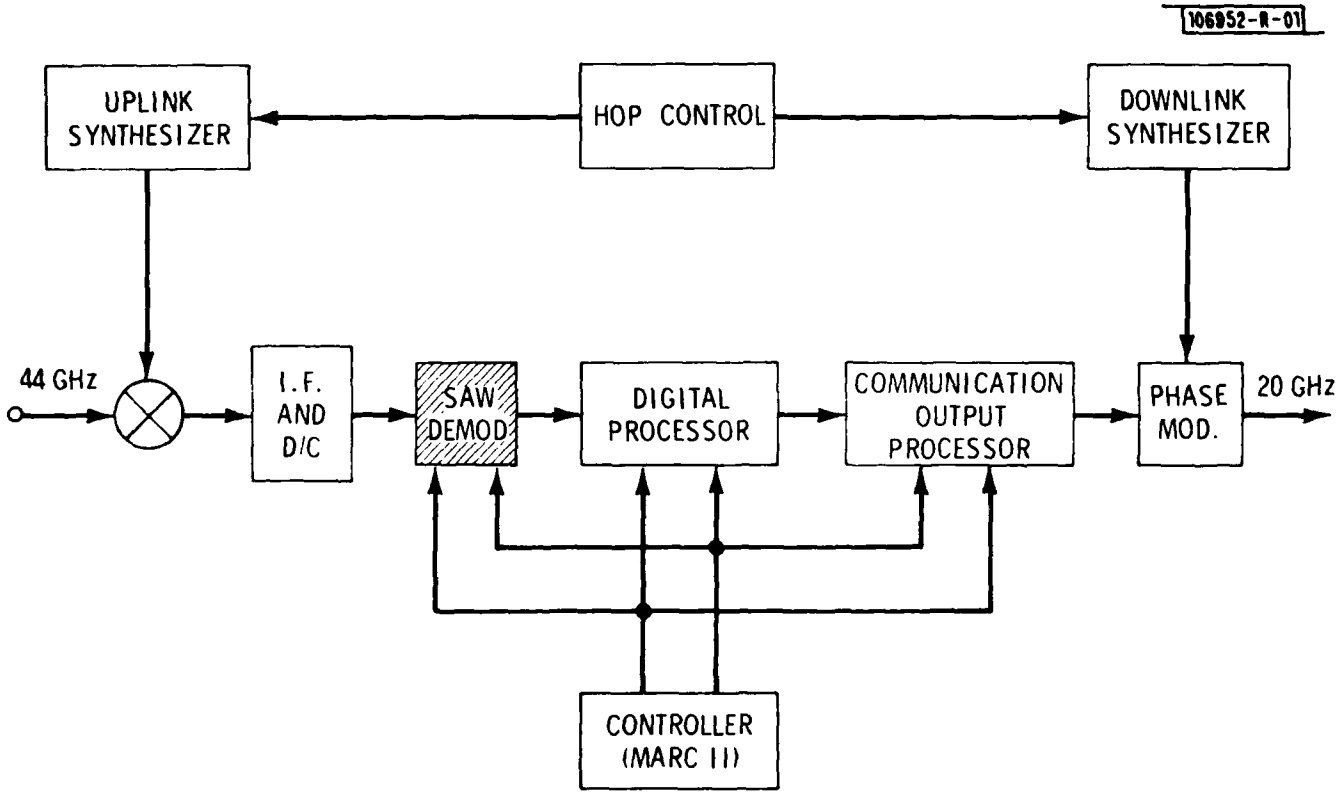

Fig. 10. Test bed payload.

controller would require new software only. The downlink formatter, or COP, would have to run at a 10 times faster output rate (roughly 8 to 10 Mbps rather than 1 Mbps as for the mobile/tactical service); however, the concept and the block diagram would be the same, and the increased rate is well within the capability of existing integrated circuits*.

B. MCOS General Characteristics

The basic purpose of MCOS is to provide Tri-Tac compatible 16 kbps full duplex links for the GMF with high jamming resistance. The terminals are assumed to be transportable, not mobile, and to operate at EHF frequencies (20 GHz downlink, 30 GHz uplink). Since mobile operation is not required, terminal antenna sizes on the order of 6 feet diameter are acceptable, with rf transmitter power output of 100 W or so. A maximum of 9 to 12 full-duplex 16 kbps links per terminal are required.

MCOS service is required typically over a coverage area 500 nautical miles in diameter, corresponding to a 1.5° spacecraft antenna beam. Within such an area, a capacity of 100 full-duplex circuits per spacecraft would be required. It is interesting to note that such service requires spacecraft EIRP comparable to that currently assumed for mobile/tactical service to terminals with smaller (2-foot) diameter antennas. The larger antennas acceptable for MCOS roughly balance the higher required data rate.

*Nearly all of the internal circuitry of the COP runs 30 times slower than the required output rate in any case, because downlink bits are retrieved from buffer memory in long words and then shifted out one bit at a time. Thus only the output shift register runs at full rate.

C. Desirable MCOS Technical Features

Full duty-cycle frequency-division multiple access (FDMA) seems more desirable than a time division multiple access (TDMA) on the uplink in order to avoid the need for very tight control and timing coordination between users, and to obtain good anti-jam performance without requiring pulsed average power limited transmitters. Time-division-multiplexing (TDM) could be used to combine multiple (up to 12) 16 kbps data streams into a single bit stream modulating a single carrier per terminal. It is also desirable to have a choice of three or so different uplink data rates (corresponding, for example, to 1,4, or 12 16 kbps channels per carrier) in order to adapt to varying levels of jamming and/or atmospheric attenuation. Control is simplified if enough uplink demodulation channels are provided at each of these available uplink rates so that their combined data equals the downlink data rate. As will be seen, such uplink channels are relatively cheap to provide by using appropriate surface acoustic wave (SAW) devices, configured in a related but somewhat different way from that used with tactical terminals operating at lower rates. On-board detection and reformatting permits TDM of all uplink signals on a single downlink carrier essentially eliminating intermodulation noise, and channel-to-channel coupling, while realizing maximum DC to rf power conversion efficiency with a given high power amplifier. Finally, there is no reason to use a hop rate different from the mobile/tactical users. The frequency-following jammer considerations are similar; moreover, such commonality would preserve the option of sharing the front-end and frequency synthesizer if architectur.. considerations led to meeting MCOS and mobile/tactical needs on the same spacecraft.

D. Strawman Uplink Demodulator Design

The basic characteristics of a strawman uplink demodulator design which has the desirable features of Section B are summarized in Table III and Fig. 11. An important feature of the design, explained in more detail below, is that the uplink timing only needs pre-correction by the terminals to a precision of about 2 to 5 μs, even though the individual signal elements themselves are as short as 2 μs. The surface acoustic wave devices are the key element in the demodulator making detection and FDM to TDM conversion possible. A description of SAW devices and the associated technology are discussed in Section H.

Each of the SAW processors in Fig. 11 employs a new configuration using five SAW devices which can demodulate many FDMA users with independent frequency and timing control, and needs only one sampler. The basic idea is to use the five SAW devices to convert FDM bit streams into a TDM bit stream (i.e., FDM/TDM converter) followed by a single matched filter set which processes all the bits of all the users sequentially. Thus, the new system does everything the Lincoln Laboratory UHF group demodulator did a few years ago, but at much higher hopping and data rates. Although motivated by the requirements of MCOS-type systems, the SAW configuration presented here should be applicable to a broad class of medium data rate systems.

A block diagram of this medium data rate, or multiple bit per hop SAW processor is shown in Fig. 12. The FDMA users are processed by the first two devices exactly as in the Current System configuration of Fig. 13; namely, they are differentially delayed by SAW dispersive delay lines (DDL), or

TABLE III

STRAWMAN MCOS PROCESSOR CHARACTERISTICS

Circuit data rate	- 16 kbps
Number of circuits	- 200 at each of 3 rates for 12, 4, or 1 circuit(s) per carrier
Modulation	- PC SFSK
Code rate	- 1/2(end-to-end)
Timing error	- $\leq$ 5% of hop period
Frequency error	- $\leq$ 75 kHz

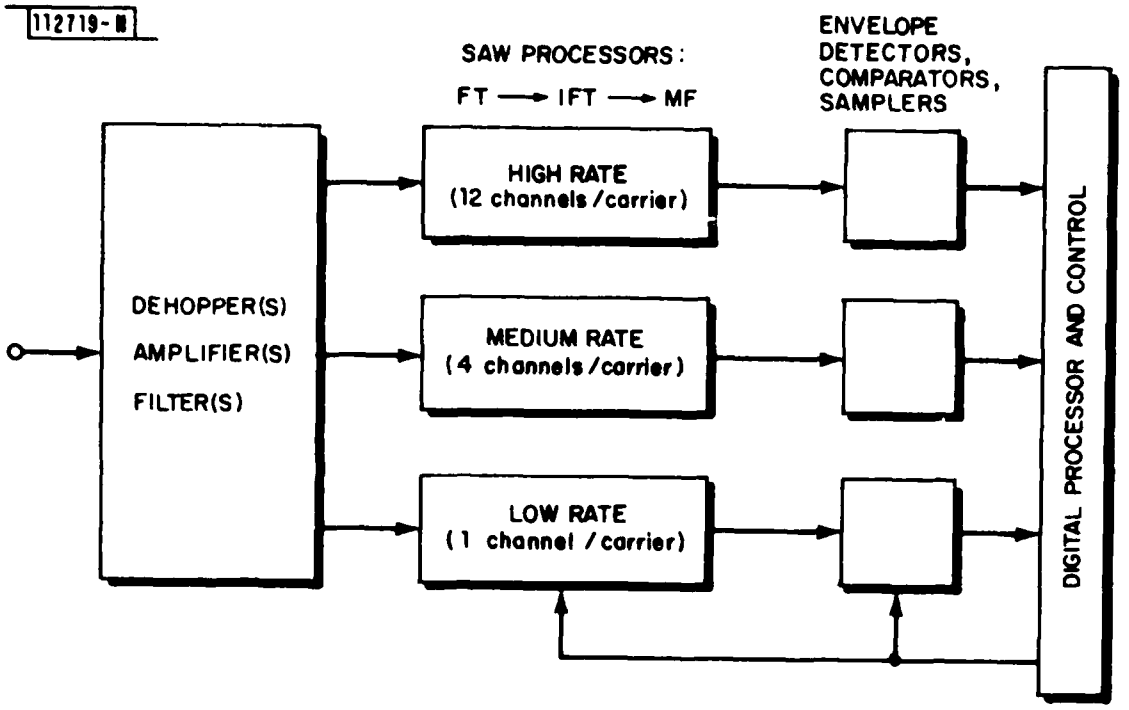

Fig. 11. MCOS demodulator.

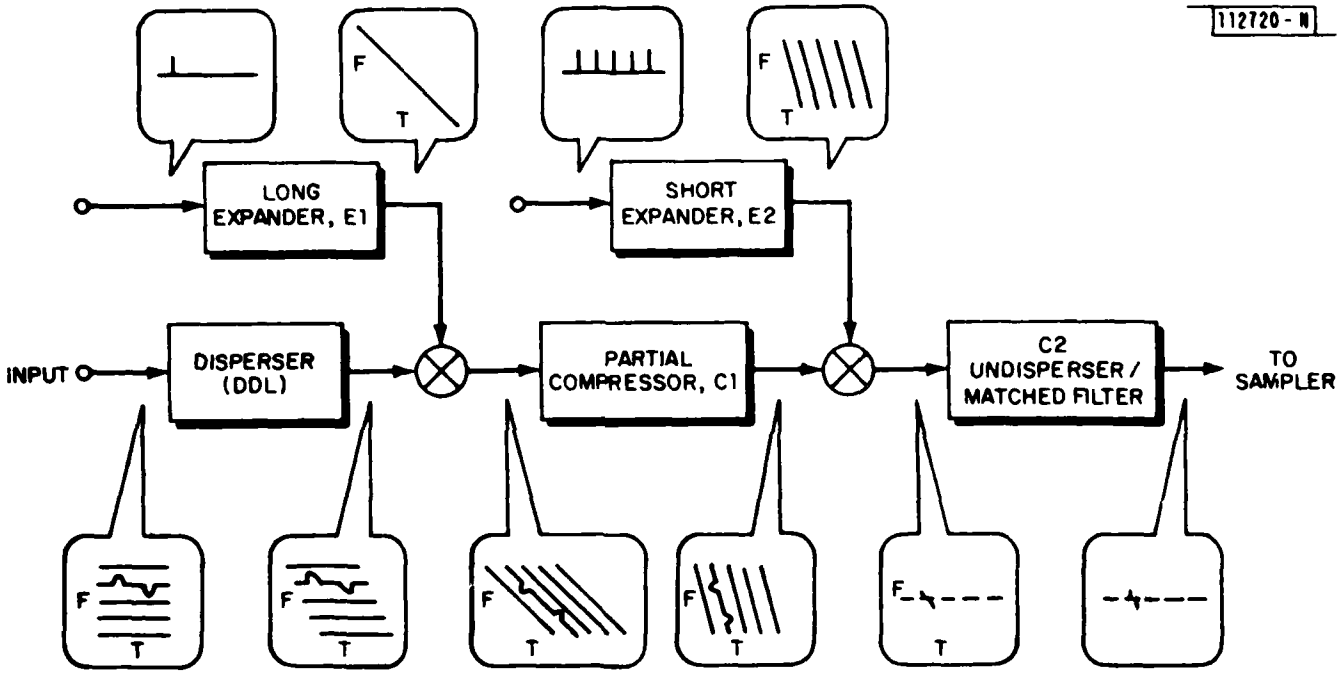

Fig. 12. Multiple-bit per hop SAW processor.

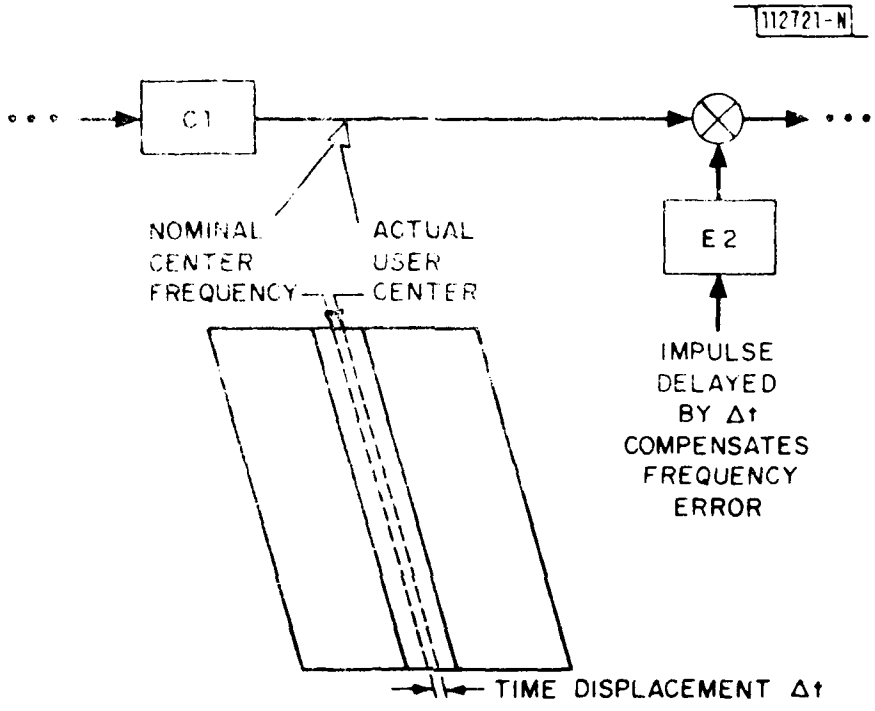

Fig. 13. Lincoln Laboratory current system SAW processor.

disperser, and then expanded by E1, the long expander, another "down-chirp" SAW device (decreasing frequency with time). The third device is an unwindowed up-chirp (increasing frequency versus time) partial compressor (C1). However, it differs from the Current System compressor in that it has a chirp slope which is not matched to the chirp slope in E1. Thus each user down chirp is made steeper so that user signals do not overlap in time. This is an important and main step since it permits the frequency and timing of each user to be independently adjusted.

The next to last step in the FDM/TDM conversion is to mix this array of down chirps with the output of a short duration down-chirp from the short expander (E2). This is repeated for each user signal. All users signals are now in proper timing sequence and at the same "center" frequency. Finally, the last up chirp device (C2) corrects the unwanted dispersion.

Notice that a user whose center frequency is incorrect appears at the output of the partial compressor (C1) as a down chirp displaced in time (see Fig. 13). User frequency error can then be corrected by an appropriate change in the time origin of the short expander (E2) chirp associated with that user.

Once the FDM/TDM conversion has been completed, the signals may be demodulated by passing them through a single set of matched filters. For instance, a stream of BPSK signals is passed through two two-bit long matched filters, one matched to no phase transition and one matched to a 180° transition. The outputs of the matched filters are then envelope detected (for example) and sampled. (Remember that the bit rate at the output of the processor is much greater than any user's input bit rate.) We can note here

that the final compressor and the matched filter could be combined into a single "chirped matched filter". Similarly, the matched filters, very short devices, could be incorporated into output transducers on the final compressor.

User bits not properly synchronized with the satellite will appear in the output TDM stream shifted in time an amount proportional to the bit timing error. Similarly, a user whose frequency error has been corrected by shifting the short down chirp appears in the TDM stream shifted in time. Thus, a single sampler can correct for known timing and frequency errors.

To say all this in another way, the output statistics of the first user all appear sequentially, then all the statistics of the next user, etc. These statistics can be examined to determine the frequency and timing error of each user bit stream and by how much the timing of the E2 input pulses must be changed to bring all users into adequate timing synchronization and frequency harmony.

In a medium-to-high data rate, frequency-hopped system, it may be desirable that each user need only be synchronized to within a fraction of a hop time (say, ± 10%). With this restriction, the user would send data for only part of each hop (e.g., 80%) so that, even if it transmitted with the worst allowable time error offset, each user data would appear at the output of the frequency dehopper. (Notice, that only the first 10% of a hop or the last 10% of a hop may be lost, but not both. Thus, a coding scheme - such as simple repetition - could be used to allow 90% of a hop to include real data.)

It is also preferable that the demodulator be forgiving for any time offset in this allowed range. That is, if all the data is presented to the demodulator, it is desirable to be able to measure the timing error, compensate for it, and perhaps request the terminal to compensate for this measured timing offset in the future transmissions. The system as described above, therefore, lets each user transmit signals during the center 80% of a hop period. His individual time offset, modulo one bit, can be found by searching for the peaks in the matched filter output using any of several early-gate-late-gate-type search strategies. After determining the measured time offset, appropriate compensation permits the data to be demodulated accurately. It is also possible to devise a scheme whereby coarse synchronization (the data bits are in the center 80% of the hop) can be obtained. For example, suppose a user transmission is a few bits late. By setting a threshold, it should be possible to determine which output sample corresponded to the first real bit and thus the time offset is determined. The user could then be informed of his error so that he could compensate for it.

Another example of timing acquisition would use a PN sequence which could be compressed by a single dedicated SAW device. The output would then have a sharp peak corresponding to the actual time offset. Such a scheme could be used in a one-shot timing acquisition system which could reclaim even more of a hop period for data transmission.

A frequency error appears as a change in the shape of the matched filter output. For a particular modulation form and bit sequence, this change may be diagnostic. If not, use can be made of the fact that a frequency error

corresponds to a time offset in the down chirp of this signal at the output of the first mixer. For example, an appropriate special-purpose SAW compressor whose output signal appears as an impulse would measure a time delay proportional to the frequency offset of the input signals.

E. Parameter Choice

There are basically only two parameters to choose other than the device center frequencies - namely, the slope of the chirp produced by E1 and by E2 in Fig. 12. It can be shown that these chirps can be completely specified by the desired compression factors. Suppose the entire TDM bitstream from one hop dwell time, T_h, must appear at the output of the FDM/TDM converter in a total time αT_h and that correction is required for frequency errors that are a fraction $\pm (1-\beta)/2$ of the inter-user frequency spacing as shown in Fig. 14. Bandwidths and dispersions of the various SAW devices are given in Table IV in terms of α and β. It is assumed that N FDMA users occupy a total bandwidth B_{total}.

The difficult problem of choosing the center frequency of each device has not been addressed. Suffice it to say that this question warrants careful study for each application. Furthermore, the choice of up or down chirp devices is a function of the chosen center frequencies. For some system designs, it may be necessary to invert the spectrum prior to detection.

An MCOS-Type Example

We have chosen to illustrate a typical demodulator with an example inspired by MCOS-type user requirements. The design parameters given here are not to be interpreted as a proposed MCOS system design. Rather, values were chosen to make many system performance characteristics suitable for a MCOS-type system.

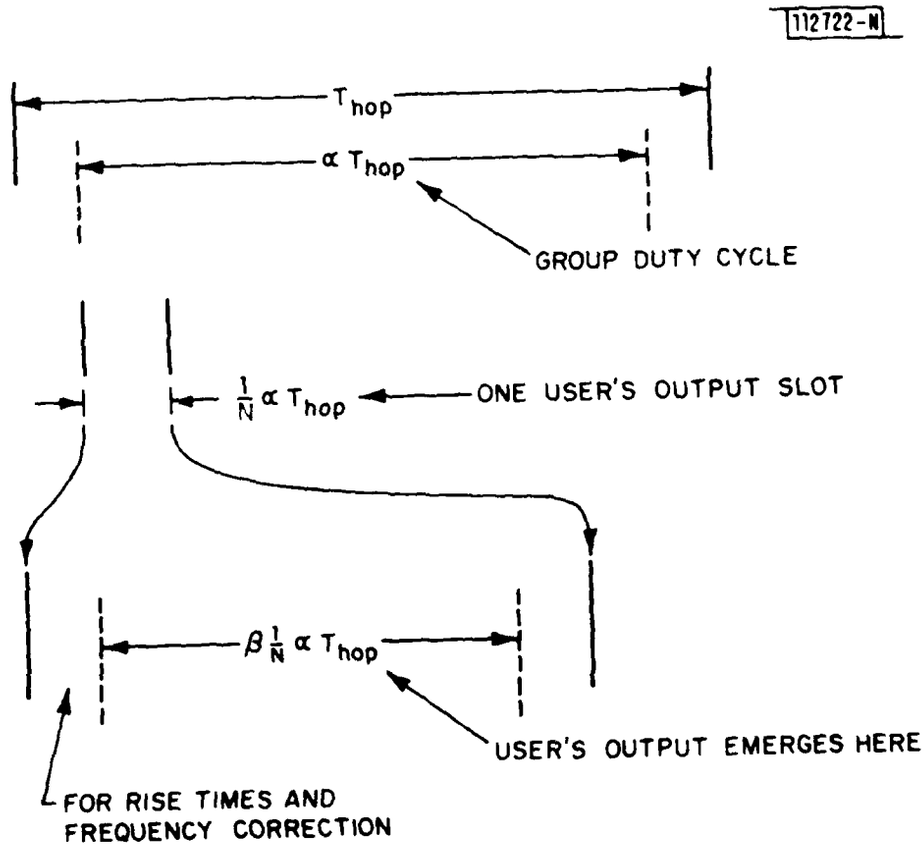

Fig. 14. Processor output structure.

TABLE IV

FUNDAMENTAL DESIGN PARAMETERS

Device No.	T/T_h	B/B_{total}
1)	α	1
2)	$1 + \alpha$	$1 + \frac{1}{\alpha}$
3)	$1 - \frac{\alpha\beta}{N}$	$\frac{1}{\alpha}$
4)	$\frac{\alpha}{N}(1 + \beta)$	$\frac{1 + \beta}{\alpha\beta}$
5)	$\frac{\alpha}{N}$	$\frac{1}{\alpha\beta}$

Each user will be assumed to send a maximum of 192 kbps of uncoded data. Such a signal would be made up of twelve 16 kbps users time-division-multiplexed on a single carrier. With rate 1/2 coding and a plausible hopping rate, there are 24 coded bits/hop/user. An additional 2 bits/hop/user are allocated for net control. Since an SFSK signaling scheme with phase comparison detection is assumed, two overhead bits per hop are required, and each user needs a total of 28 channel bits/hop. Assuming an allowable time offset of ± 6.25% of a hop, these 28 channel bits must be sent in 54.7 μs, or at a signaling rate of 512 kbps. Thus there are 32 total channel bits in a hop including the two prefix and two suffix bits, which may be used for timing or frequency acquisition, or some other purpose.

The center frequencies are spaced at $\Delta_f/R = 2.5$ giving each user a bandwidth of 512 x 2.5 = 1.28 MHz. Assuming 17 users results in a 21.76 MHz communications bandwidth. These design values are summarized in Table V, along with similarly-derived numbers for four and one 16 kbps circuits/carrier, respectively.

As in the Current System design, there is a tradeoff to be made between the rate of the demodulator's output comparator period and the maximum time delay of the longest SAW device. Specifications of the SAW devices required for the three demodulators are given in Table VI.

As shown in the table, it is possible to get reasonable values for the required output comparator response period (25 to 80 ns) with long-expander (E1) dispersion values of 109 to 112.5 ms. These values are somewhat beyond what is convenient for a single SAW device but can be readily realizable with

TABLE V

MULTI-RATE SYSTEM DESIGN

No. of 16 kbit circuits	12	4	1
No. of coded bits/hop (R=1/2)	24	8	2
Phase comparison overhead bits	2	2	2
Control overhead bits	2	2	1
Extra timing overhead bits	4	2	0*
Total channel bits/hop	32	14	5
Allowable timing offset	± 6.25%	± 7.17%	± 10%
Signaling rate	512 K	224 K	80 K
BW/user ($\Delta f/R_{channel}$=2.5)	1.28 M	560 K	200 K
No. of Channels	17	50	200
Total BW	21.76 M	28 M	40 M
Overhead	1.25 dB	2.43 dB	4.0 dB

TABLE VI

SPECIFICATIONS OF SAW DEVICES FOR THREE MCOS DEMODULATORS

No of 16 kbit circuits/channel	12			4			1		
Frequency error allowed	± 64 kHz			± 70 kHz			± 50 kHz		
Timing error allowed	± 6.25% of hop			± 7.1% of hop			± 10% of hop		
Output comparator period	80 ns			50 ns			25 ns		
	T(μs)	B(MHz)	TB	T	B	TB	T	B	TB
Dispersive delay line	48.36	21.76	1,052	46.7	28	1,307	112.5	40	2,000
Expander 1[a]	110.86	49.89	5,531	109.2	65.5	7,150	112.5	90	10,125
Partial compressor	59.94	28.13	1,686	61.8	37.5	2,318	62.38	50	3,119
Expander 2[b]	5.4	59.38	320	1.63	87.5	143	.375	150	56
Undisperser[b,c]	2.84	31.25	89	.93	50	47	.25	100	25
Matched filters[c,b]	.24	31.25	7.5	.15	50	7.5	.075	100	7.5

[a] constructed of 2 shorter expanders in cascade
[b] may use SAW device other than RAC
[c] may be combined into single device

two devices in cascade. For comparison, the specifications of the SAW devices in the existing Current System Test Bed Hardware are summarized in Table VII.

F. Simulation Results

The MCOS-type demodulator was evaluated using a computer simulation* that models the transfer characteristics of the SAW devices, especially near the edges of their operating frequency bands. All devices were assumed to have a quadratic in-band phase response.

A detailed report of the performance characteristics is not important here; suffice it to say, the demodulator performed as expected providing FDMA/TDMA conversion with a tolerable phase and amplitude distortion. This new configuration of SAW devices does indeed demodulate FDMA high-rate, multiple-bits-per-hop users. The system allows for independent time and frequency error correction by converting the FDMA signals into a TDM stream which requires only one set of high rate matched filters. This specific system using PCSFSK modulation was inspired by GMF/MCOS requirements.

G. Summary

The foregoing describes the general and specific characteristics of a particular type on-board signal processor; that is, one which converts the input (uplink) FDM signals into a TDM output bitstream. It is particularly significant in that the SAW devices have a time-bandwidth (TW) product sufficiently high to accommodate 100 duplex 16 kbps channels with frequency

*The actual numbers used in the simulation differ modestly (~ 20%) from the final strawman design values of Tables VI and VII. This is unimportant for demonstrating the validity of the concept.

TABLE VII

SAW DEVICE CHARACTERISTICS
(LINCOLN LABORATORY CURRENT SYSTEM TEST BED)

	Center Frequency	T	BW	TB
Disperser	100 MHz	33.6 μs	15.2 MHz	511
Expander	250 MHz	81 μs	36.6 MHz	2965
Compressor	150 MHz	47.5 μs	21.4 MHz	1017

hopping. Higher data rates and/or more channels might be accommodated by either increasing the TW product, or alternatively by paralleling and cascading the SAW devices with TW product equal to, or less than those described here. The latter may be preferred especially since the devices described in the strawman processor have TW products about as large as can be achieved with current technology.

Clearly, the SAW device and its performance characteristics determine, to first order, the throughput communication capacity. Consequently, it is appropriate to discuss the general characteristics and fundamental limitations of this device and indicate its current state-of-the-art performance and characteristics.

H. SAW Devices

The device consists of a pair of acoustical transmission lines along which frequency selective reflecting obstacles are distributed. Electrical signals, at frequency f_e, excite corresponding acoustic signals at frequency $f_a=f_e$ that propagate along the surface acoustical wave input transmission line. When the induced acoustic wave encounters a "resonant" obstacle (resonant at f_a), it is reflected (coupled) to the output acoustical wave transmission line and propagates essentially unattenuated to the output transducer where it is converted to an electrical signal at f_e. The total propagation delay τ_a is equal to the time required for the signal to propagate from the input tranducer to the frequency selective reflecting objects and then to the output transducer. Since the propagation velocity of the surface acoustical wave is essentially independent of frequency, signals at frequency

f_l, $f_l \neq f_a$, travel a longer, or shorter, distance prior to reflection by obstacles tuned at f_l. If the distance is longer for $f_l > f_a$ signals at frequencies higher than f_a undergo a time delay greater than τ_a and signals less than f_a undergo a time delay shorter than τ_a. Hence the SAW device has positive frequency versus time slope (i.e., up chirp) in that higher frequency signals arrive at the output a later time τ_l approximately in proportion to the difference between the higher and the lower frequency. That is,

$$\tau_l \approx \tau_a + \alpha(f_l - f_a) \quad . \tag{6}$$

It follows that the differential time delay τ at any frequency in the operating frequency band, W, is given by

$$\tau = (f - f_\ell)\alpha \tag{7}$$

where f_ℓ is the lowest frequency in W. The maximum time delay τ_m is given by

$$\tau_{max} = (f_m - f_\ell)\alpha \tag{8}$$

where f_m is the highest frequency in W, and $W = f_m - f_\ell$; hence

$$\tau_{max} = W\alpha \quad . \tag{9}$$

Now τ_{max} is limited to about 100 μs because current technology does not permit the manufacture of acoustical transmission lines long enough to introduce a 100 μs delay and operate at a frequency, f_o, sufficiently high to accommodate W. That is, the ratio f_o/W should be greater than say three. It follows that W can be increased by increasing f_o; however, current technology requires that f_o be less than about 3 GHz. Bandwidth and τ_{max} of currently available SAW devices[6] (also referred to as Reflective-Array Compressor, RAC) are shown in Fig. 15. Notice that the TW product is less than about 10^4 (Hz-s); larger TW products can be accommodated by cascading and/or paralleling one, or more, SAW devices.

Table VII lists the characteristics of SAW devices used in the Lincoln Laboratory Current System Test Bed Hardware. These devices can be used in spacecraft applications. Performance (i.e., larger TW products) significantly greater than that given in Fig. 15 is beyond fundamental limitations of the device. Although, current fabrication techniques are limited to special laboratory facilities, future R&D efforts should support transfer of these processes and/or facilities to the industrial or manufacturing base.

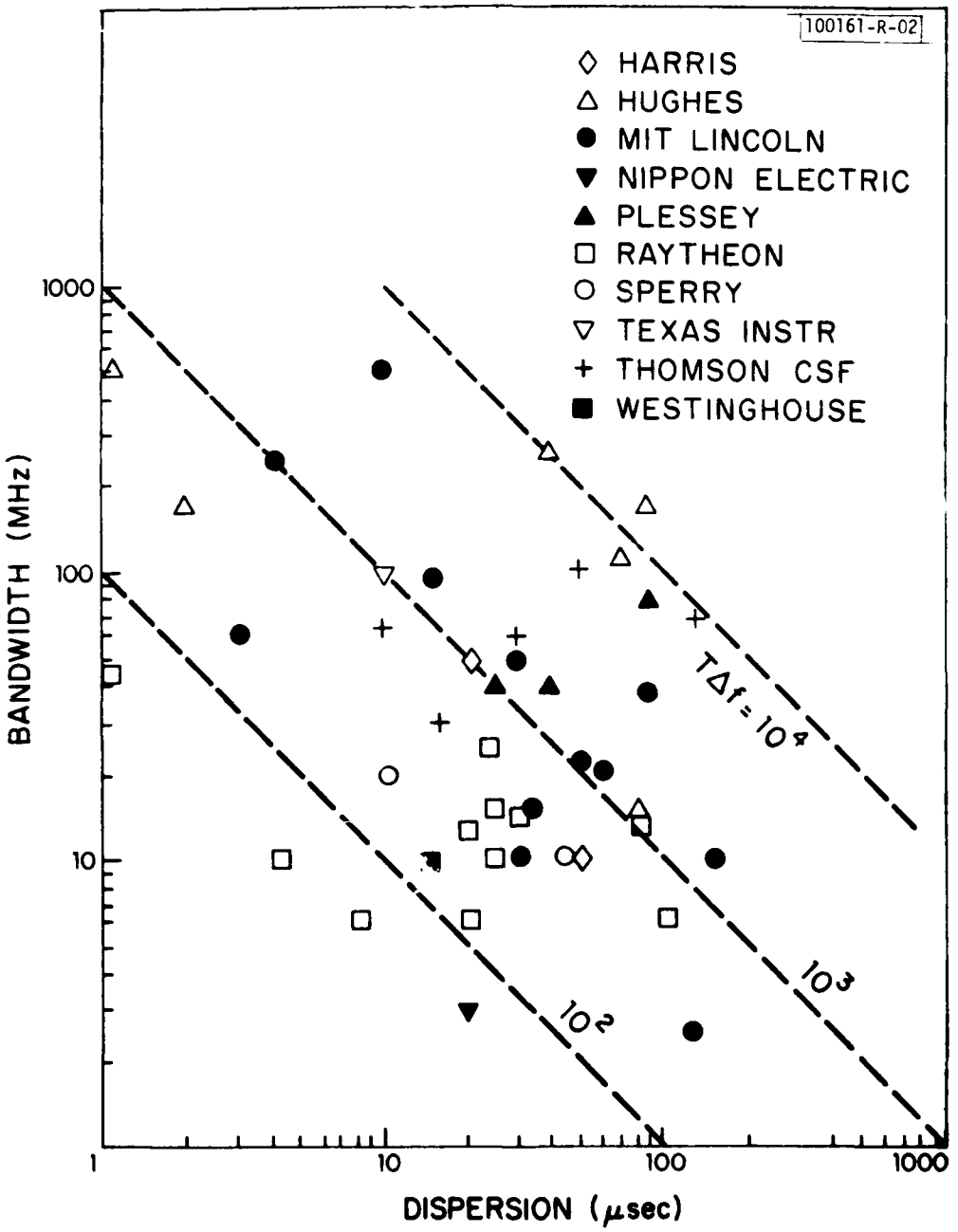

Fig. 15. Capacity of reflective-array compressor.

IV. RADIATION EFFECTS

A. Introduction

In the natural environment, particles ranging from electrons to heavy cosmic rays continually bombard spacecraft. These particles have various sources and energies and populate different regions of space. While some penetrate only the outer micron of a satellite's skin, others pass completely through spacecraft, leaving a trail of damage in their wake. Their effects on electronic components and systems vary substantially with device technology and design. Indeed, expected component lifetimes in space can vary from days to decades depending on component technology, shielding, and orbit.

The purpose of this section is to present radiation-hardness guidelines for selecting parts to be used in satellites and to assess the hardness of currently-available components against those guidelines. The scope of the assessment is limited principally to the natural space environment, dominated at synchronous orbit by trapped electrons and solar-flare protons. It does not include nuclear-blast radiations nor the enhanced trapped radiation present after high-altitude bursts.

The radiation hazards of the natural space environment are summarized here in a manner useful to the engineer concerned with spacecraft electronics. The sources of natural radiation, from the low-energy thermal plasma to relativistic cosmic rays, and the physics of their interaction with electronic materials are discussed briefly, and realistic hazard levels are assessed as a function of shielding thickness for several common orbits.

With the hazard levels clearly in mind, radiation susceptibility of electronic components that are potentially useful for spacecraft systems is addressed. General characteristics of generic device technologies then follow from specific test results obtained at Lincoln Laboratory as well as from other data published over the past few years in the technical literature. Finally, ongoing programs to develop radiation-hardened components are discussed, and a few suggestions for future program funding are offered.

B. Sources

The primary radiation hazard in earth orbit comes from the Van Allen radiation belts, intense regions of energetic electrons and protons confined by the Earth's magnetic field. The single proton belt peaks at roughly 2,000 nmi altitude in the equatorial plane for proton energies in excess of 20 MeV, with densities dropping to about 1% of peak at 500 and 5,000 nmi, respectively. Electrons are confined to two broad regions, peaking in the 5,000 to 10,000-nmi altitude range, with significant densities extending from about 2,000 nmi out to geostationary orbit. Trapped by magnetic field lines, the particle distributions tend to peak in the equatorial plane with most confinement between 45°N and 45°S latitudes. Within these belts, particle densities decrease exponentially with energy (i.e., with trapped energies extending up to 100 MeV for protons and to 6 MeV for electrons). The relatively sparse high-energy tails to the distributions contain the particles that are capable of penetrating spacecraft shielding and affecting electronic components.

Significant fluxes of energetic protons and alpha particles, originating in solar flares, penetrate the earth's magnetic shield, particularly in high earth orbits (geosynchronous) and in polar regions. The most damaging solar-flare particles occur sporadically. Indeed, a single short-lived solar flare can produce most of the yearly fluence of such particles. In estimating their fluence, probabilistic models depending on the solar cycle are used, and only long-term ($\geq$ yearly) averages are reliable.

Cosmic rays of galactic origin have recently been recognized as a significant radiation concern for satellite electronics. The particles are light nuclei ranging up to iron in atomic number. They are accelerated to relativistic energies in excess of 1 GeV per nucleon by interstellar magnetic fields. Although fluxes are low, cosmic rays penetrate any practical spacecraft shielding, and their effects on components must be accommodated by appropriate system design.

At the low end of the energy spectrum, plasma electrons and ions (mostly protons) with energies from a few to hundreds of electron-volts (eV) constantly engulf satellites in earth orbit. Penetrating only microns into the skin of the spacecraft, these particles usually have no effect on electronic systems. However, in higher orbits, (particularly near synchronous), geomagnetic substorms can disturb the quiescent particle-energy distributions and inject significant numbers of 10 to 20 keV electrons which impinge on satellite surfaces at current densities up to several nA/cm^2. Combined with a photoemission clamping current from sunlit surfaces, plasma electrons can charge spacecraft surface materials to potential differences of

several thousand volts, leading to electrical surface breakdown. Both radiated EMI and direct current injection from such discharges can couple into spacecraft systems, causing logic upset and possible component damage.

C. Effects of the Space Environment

The predominant natural radiation hazards in synchronous orbit are trapped electrons ranging up to about 6 MeV in energy and solar protons ranging from about 20 to 100 MeV in energy. In orbits which penetrate the radiation belts (e.g., 12-hour elliptical, 6-hour orbits, or low orbits above 1,000 nmi) trapped protons up to 100 MeV are significant, and can dominate the dose.

Shielding is relatively effective at stopping the electrons, but much less so for the protons. In devices, both particle types cause ionization damage (generation of electron-hole pairs) and bulk displacement damage (lattice vacancies and interstitials), but in very different proportions. Electrons lose energy almost entirely by ionization, while protons are effective in producing both forms of damage. Bipolar devices (minority carrier operation) are sensitive to bulk damage, leading to reduced carrier lifetimes, diffusion lengths and hence degradation of current gain, β. FET devices (majority carrier operation) are relatively insensitive to bulk damage but are quite sensitive to ionizing radiation. This leads to trapped charge in oxides and therefore to shifts in both surface doping levels and effective threshold voltages. Trapped charge (from ionization) in field oxides can cause surface leakage currents in both device types.

In determining device radiation sensitivity, the effects of ionization and of bulk displacement must be distinguished. The measure of ionizing

radiation is the total ionizing dose (TID), or simply total dose, in units of rads (1 rad → 100 erg/gm deposited energy in the specific material). One rad (silicon) is approximately equal to the dose produced by 3×10^7 e/cm^2 at an energy of 1 MeV.

Bulk damaging radiation is measured in terms of DENIs (Damage-Equivalent Normally Incident electrons), the fluence of normally incident electrons which produces the equivalent bulk damage in the material under test. Another name for this measure is the BDEF, for Bulk-Damage-Equivalent Fluence. Historically, this 1 MeV equivalent fluence has served as the transfer standard for expressing the bulk-damage effects of residual electron and proton spectra penetrating shielding. Another measure of device susceptibility related primarily to bulk damage is the total neutron-fluence damage threshold, commonly used in nuclear-effects tests.

As an environmental radiation-simulation tool for bulk damage, 1 MeV electrons must be used with some care, since they will produce not only the specified bulk damange but also a concomitant amount of ionization. Note that for an electron-radiation hazard, the two effects are simulated well with electrons. However, for a proton-radiation hazard, the electron fluence required to simulate the expected bulk damage in test devices will generate a substantially greater TID than would actually occur in orbit.

D. Accurate Determination of Exposure

Determination of the TID or BDEF expected at a specific location within a spacecraft on a particular mission involves a 2-step procedure. One first determines the external environment by integrating environmental models (i.e.,

particle-flux spectra as a function of magnetic coordinates) over the particular orbit. Second, one calculates the TID in rad or BDEF in e/cm^2 which results from the specific environment penetrating the mechanical shielding of the spacecraft structure. Accurate treatments require a computer data base representing the environmental model, a computer program to convert geocentric orbit parameters into magnetic B-L coordinate space, and a program to integrate the environment over the orbit. This procedure yields the time (orbit)-averaged energetic-particle spectral flux external to the spacecraft due to trapped particles. The expected solar-proton fluence for the time period of interest is determined separately from existing models.

Monte Carlo-type codes are generally used to convert this spectrum to TID and BDEF at specified points inside the spacecraft, given a computer model of the structural configuration and materials. Such shielding programs range from relatively simple ones assuming a spherical-shell geometry of uniform thickness (requiring several minutes of computer time) to complex ones allowing more than 100 surfaces (requiring several hours of computer time).

Programs for shielding calculations must take into account bremsstrahlung radiation generated in stopping energetic electrons. In the bremsstrahlung interaction, a primary incident electron colliding with a nucleus of the shield material has some or all of its energy converted to a photon (or gamma ray) continuing in the forward direction. The resulting bremsstrahlung gammas are extremely penetrating and will limit the effectiveness of shields thick enough to extinguish all primary electrons. The probability of this reaction taking place increases with atomic number of the target nucleus, while the

shield effectiveness against primary electrons depends only on the mass area density (gm/cm^2) of the shield. Therefore, outer shields on spacecraft should be made of materials with low atomic numbers. Aluminum is assumed in the examples which follow.

E. Depth-Dose Curves

Figure 16a shows the curves of total yearly dose through a spherical aluminum shield versus shielding thickness for the geostationary orbit. The environmental models used were AE17-HI for electrons, AP8-MAX for trapped protons, and SOLPRO for solar protons (models and computer codes provided by G. Stassinopoulos, NASA Goddard). The contribution of solar protons to total dose is small for moderate shield thicknesses; that of trapped protons is completely negligible at synchronous orbit. The limiting effect of bremsstrahlung is evident.

Figure 16b shows the corresponding annual depth-dose curve for a typical 12-hour elliptical orbit (Molniya type). The contributions of both trapped electrons and protons are substantial in this orbit, which passes through the radiation belts. The contributions of bremsstrahlung and of solar protons are relatively less important than in geostationary orbit.

In general, flat-plate models will produce smaller doses than will spherical models, since much of the isotropic radiation enters the shield at skew angles, seeing an effectively thicker shield. Note that an important consequence of the exponential dependence of dose rate on shield thickness is that thin spots (or "holes") in the shield dominate the dose. This point cannot be overemphasized.

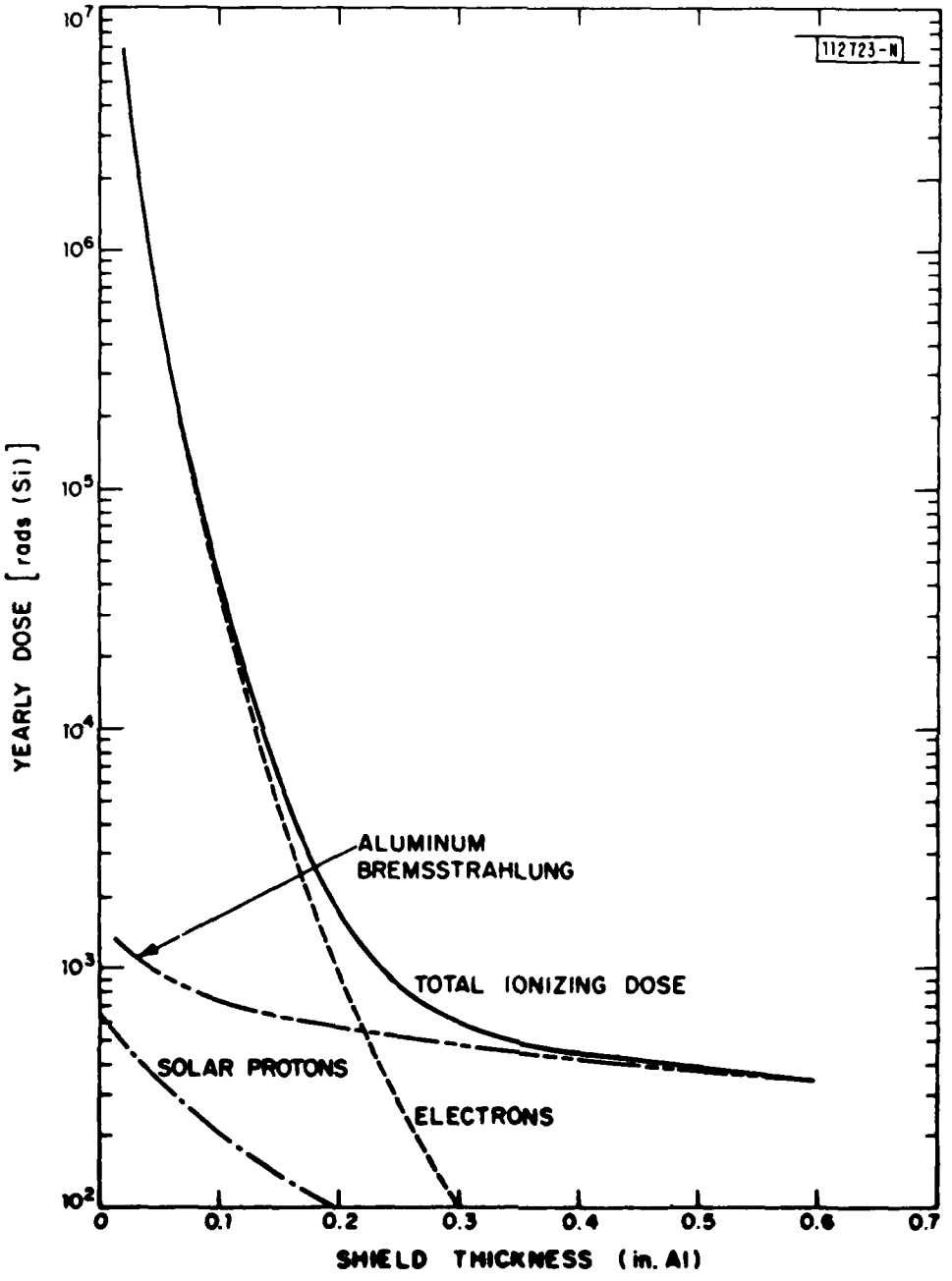

Fig. 16(a). Ionizing dose in geostationary orbit.

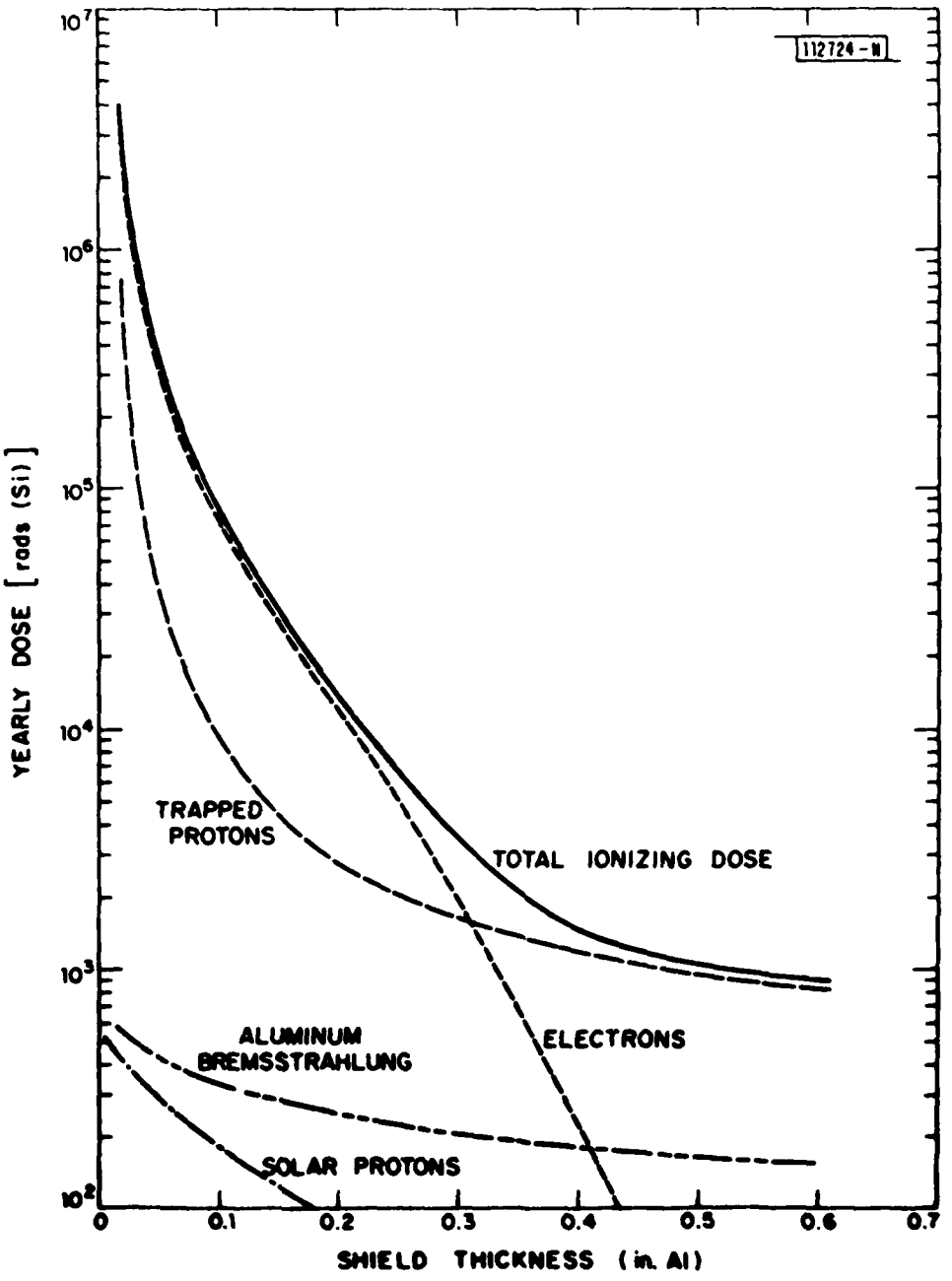

Fig. 16(b). Ionizing dose in 12-hour elliptical orbit.

Figures 17a and 17b show curves of the annual bulk-damage-equivalent fluence (BDEF) in DENIs (1-MeV damage-equivalent normally incident electrons) corresponding to the two orbits discussed above. Solar protons are far more significant for the BDEF curve than for the TID curves of a geostationary orbit, and they dominate BDEF for shield thickness in excess of 0.100-in. aluminum. The reduced effectiveness of shielding for protons as compared to electrons is apparent. The solar-proton curve shown represents the anticipated maximum solar-proton fluence for a mission in the 1983-1989 time frame. In the 12-hour orbit of Figure 17b, trapped protons completely dominate the BDEF.

F. Radiation Hardness Requirements

From the data shown in Figures 16 and 17, it is clear that — behind a nominal shield thickness of 0.100-in. aluminum — approximately 50 krad/year can be expected in geostationary orbit. In a 12-hour elliptic orbit, the equivalent dose rate is 100 krad/year, twice that of geostationary. Increasing the shield thickness to 0.200-in. lowers the yearly dose rates to 2 and 15 krad, respectively. The differences in BDEF between the two orbits are even more drastic. For the geostationary orbit, the equivalent yearly fluences through 0.100-in. and 0.200-in. aluminum shields are approximately 0.4 and 0.1 x 10^{13} e/cm^2, respectively. The corresponding fluences in the 12-hour orbit are 4 and 1.4 x 10^{13} e/cm^2, roughly an order of magnitude greater than at geostationary orbit.

When determining the radiation hardness/shielding requirements for a specific mission, the dependence of end-of-life dose on orbit parameters must

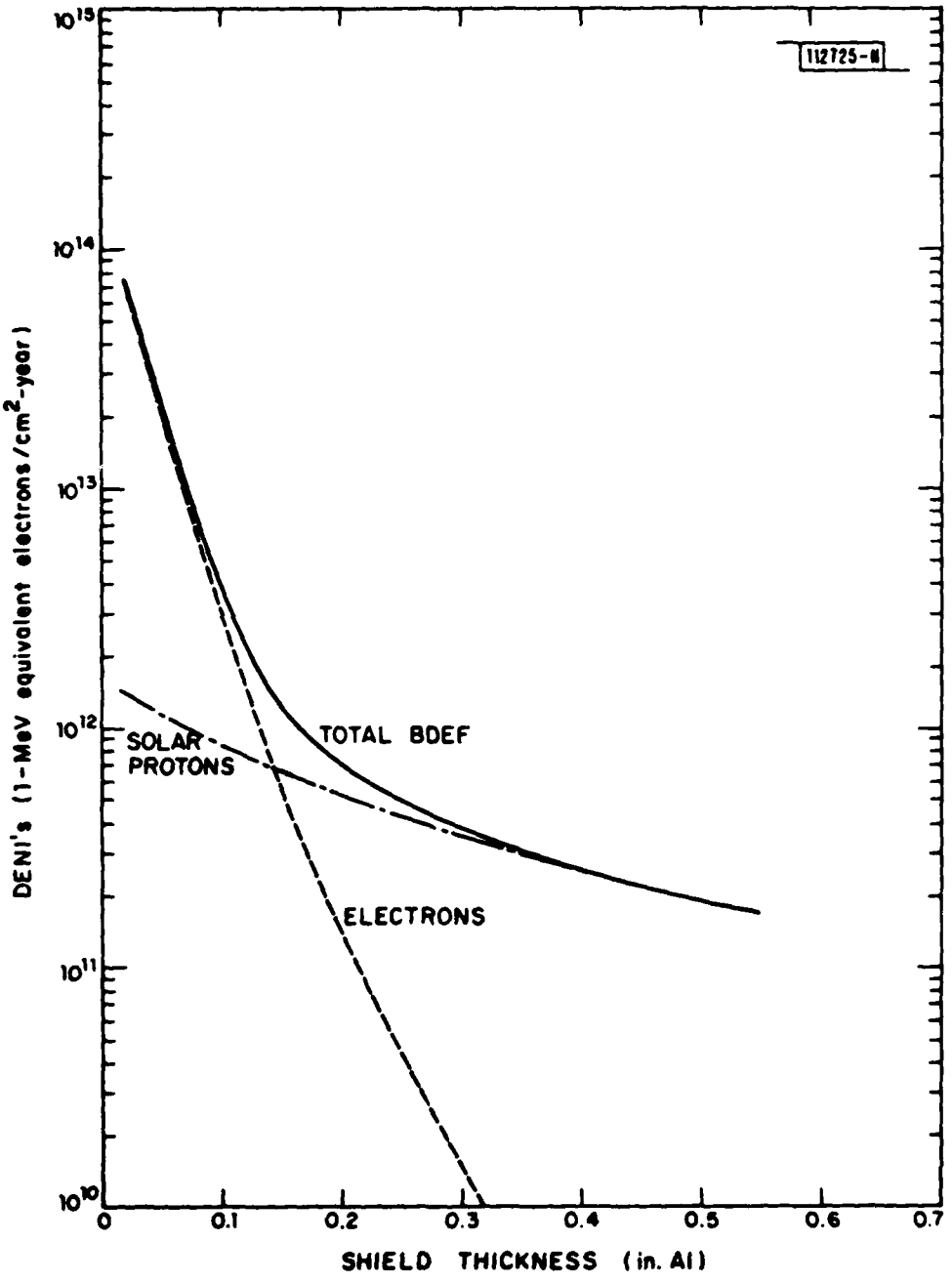

Fig. 17(a). BDEF in geostationary orbit.

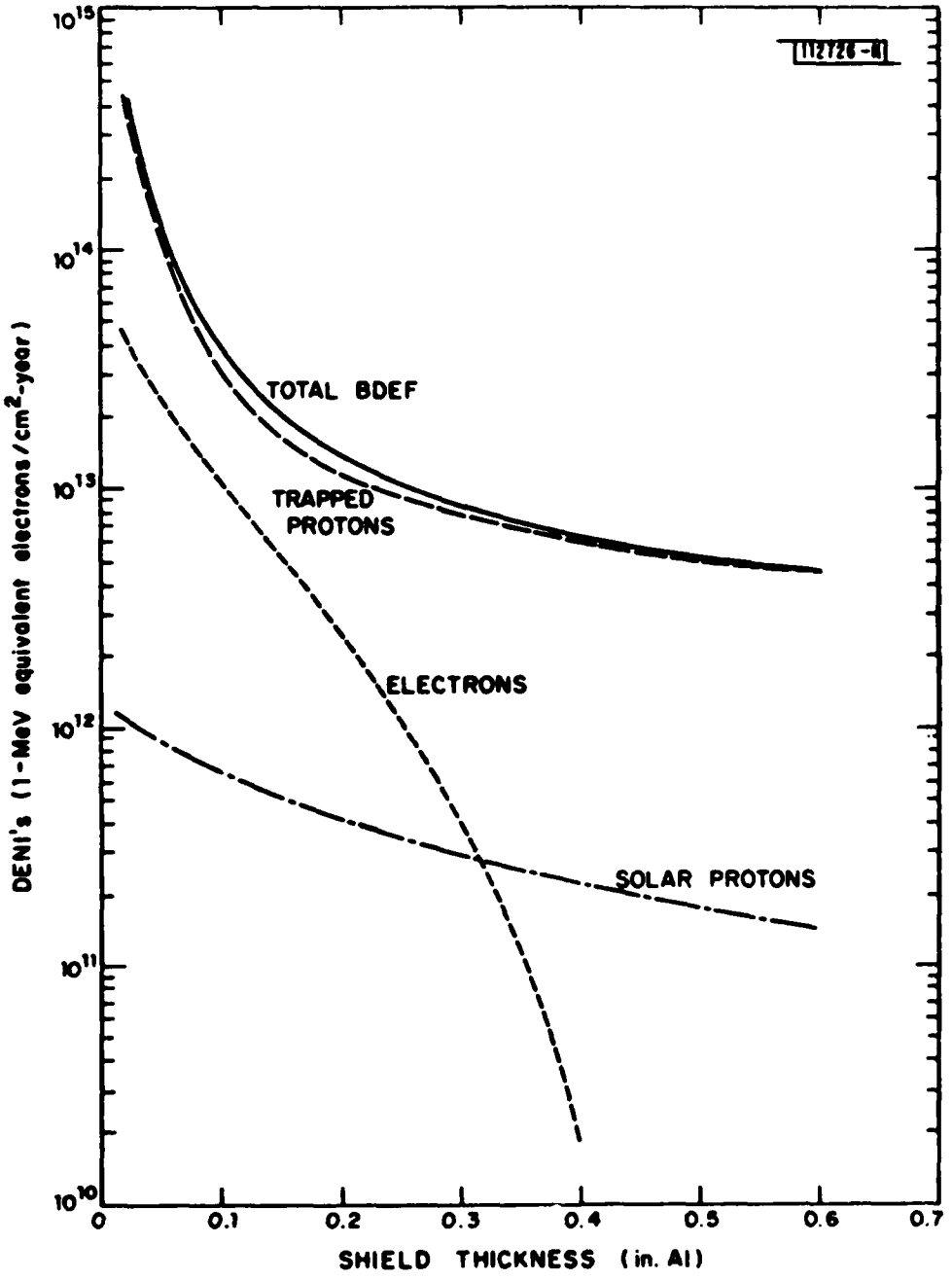

Fig. 17(b). BDEF in 12-hour elliptical orbit.

be kept in mind. One must also recognize the extent of temporal variation in dose rate. Expansion and contraction of the geomagnetic field (typical in geomagnetic storms) can carry the energetic trapped-particle regions across synchronous orbits, resulting in order-of-magnitude increases in electron fluxes at several MeV. Such increases can last for several weeks. Reasonable design margins must be allowed for temporal environmental uncertainties and for potential changes in orbit longitude.

In lieu of specific orbit parameters and structural models, some general guidelines can be extracted from Figures 16 and 17. The uniform-spherical-shield reduction of AE17-HI and the proton model for the 1983-1989 period should represent a reasonable upper limit for TID and BDEF calculations. Assuming a minimum of 0.100-in. aluminum equivalent shielding from box walls, circuit cards and outer structures, an upper-limit 10-year TID is approximately 1 Mrad. Parts hard to that level should be acceptable for flight use without much concern. Parts which degrade unacceptably at 1 Mard but which are hard to a TID in excess of 100 krad can be used, but they will require additional local shielding and judicious placement within the satellite structure. Parts which fail in the TID range of 50 to 100 krad can theoretically be shielded, but shield weight becomes excessive and shielding margin is lost. Such parts should be considered unacceptable unless compelling arguments require their use. Parts which fail below 50 krad are unacceptable.

Bipolar devices, sensitive to bulk damage, must survive a BDEF of 5×10^{14} e/cm^2 to be used without further concern on 10-year missions. Parts

which survive a BDEF of 3×10^{12} are potentially usable with appropriate shielding, depending upon the intended orbit. For bipolar devices (particularly linear devices) which cannot survive 3×10^{13} e/cm^2 because of the implied TID level (3×10^{13} e/cm^2 + 1 Mrad), effort will be required to distinguish BDEF effects from TID effects.

Note that the upper-limit exposures are based on an assumed average effective shield thickness of 0.100-in. aluminum and a 10-year mission life. The hardness guideline level for fully acceptable parts (i.e., parts useful without concern for additional shielding) will vary strongly with minimum shield thickness according to Figures 16 and 17. All levels will vary linearly with time and will depend somewhat on the environmental model used.

G. Device-Technology-Hardness Guidelines

The following general guidelines in Table VIII may be useful in selecting device technologies. Whether a specific device is acceptable at a given total dose level can depend critically on device architecture, manufacturing parameters, and circuit requirements. For marginally acceptable parts, testing is crucial. The Lincoln Laboratory Group 68 automated Radiation Test Facility (RTF) is now being used routinely to test specific devices of interest to Lincoln Laboratory's Space Communications program.

H. Specific Component Assessments

The balance of this report summarizes the current state-of-the-art of radiation-resistant components which are candidates for use in communications satellite systems. The information presented is based on results of testing performed at Lincoln Laboratory as well as elsewhere within the radiation

TABLE VIII

HARDNESS GUIDE

Technology	Expected TID Hardness	Expected BDEF Hardness
Bipolar digital IC	> 1 Mrad	> 10^{14} e/cm^2
I^2L	200 krad - 1 Mrad	?
Bipolar linear ICs		
(hardened)	> 100 krad	?
(unhardened)	< 50 krad	
CMOS		
(hard design and processing)	> 500 krad	(not critical)
(hard processing only)	~ 100 krad	(not critical)
(unhardened)	~ 10 krad	(not critical)
PMOS	~ 100 krad	(not critical)
NMOS	< 10 krad	(not critical)
GaAs	> 1 Mrad	> 10^{14}
Surface Acoustic Wave devices	> 1 Mrad	> 10^{14}

effects community. Although the current selection of radiation-tolerant LSI chips is limited, the need for long-lived, hardened microcomputer-based systems on orbit is compelling.

To meet satellite system constraints on weight, power, and reliability, we desire high-density microprocessor and memory components produced from a low-power technology. To meet the threat posed by the environment, we desire components which tolerate a total dose of at least 1 Mrad, minimizing the weight of shielding required. However, given the limits of shielding (even neglecting weight), parts must still be hard to about 100 krad in order to preserve any safety margin.

At the 100-krad level, NMOS devices, which are most commonly used by the commercial world, are completely ruled out in their current form (typically unable to withstand 10 krads). While TTL parts are adequately hard, they are generally considered to be too power-consuming for extensive systems use, particularly for memory-intensive systems. The technologies which remain as candidates for this application are hardened CMOS and possibly I^2L.

System tolerance of cosmic rays is another consideration which must be folded into component selection and system design. Tests have demonstrated the tendency of digital integrated circuits to flip bits when struck by cosmic rays, and for this effect to become more likely as LSI and VLSI parts move toward smaller device geometries. Circuit redundancy or some form of error-correction coding may be required in critical areas. Recent measurements have shown that the susceptibility of CMOS parts to cosmic rays is substantially reduced as the supply voltage is increased from 5 to 10 V. Since total-dose

tolerance in CMOS also tends to increase with supply voltage, higher-voltage CMOS parts may be preferred to the lower-voltage, TTL-compatible variety. However, other systems considerations also weight heavily in any such selection.

I. Microprocessors

Two microprocessors which are leading candidates for a flight system are the I^2L SBP 9900 ANJ (Texas Instruments) and the CMOS CDP 1802 (Sandia National Labs/RCA).

Sandia has been doing considerable work in the development of rad-hard CMOS devices. Their intent is to transfer successful technology to RCA and other commercial organizations. This apparently is not as easy as it sounds, although they seem to be having more success lately. The Sandia 1802 devices have been tested in 1.5 MeV electrons in the Lincoln Accelerator Laboratory and have achieved tolerance levels of 300 and 650 krad on devices fabricated in 1979. N. Wilkin, et al.,[7] have observed 1802s tolerant to > 280 krad, when tested with a LINAC, and E. E. King, et al.,[8] saw levels > 200 krad in 1977.

Another developmental microprocessor, the TCS-129A, is a CMOS/SOS 8-bit-slice device that was designed primarily for transient hardness.[9] Preliminary estimates indicate that it should survive 100 krad of total dose. This chip-set family is not yet commercially available.

Two I^2L microprocessors have been evaluated at Lincoln Laboratory: the Fairchild 9440 which failed at 10 krad,[10] and the Texas Instruments SBP 9900 ANJ 16-bit microprocessor, which appears to be acceptably hard. We

have tested nine of the TI microprocessors so far and have seen tolerances ranging from 200 krad to $\geq$ 1 Mrad. Hardness correlates strongly with the data code, suggesting that radiation tolerance is lot-dependent with these devices.[11] With adequate lot/wafer sampling, these devices should be available at Mrad hardness levels.

T. Ellis of Naval Weapons Support Center tested the 9900 extensively and has found total dose tolerances exceeding 3 Mrad using a cobalt-60 source.[12] Ellis has also recently tested the 9900 for cosmic-ray effects. He observed[13] soft bit-flips in both the 9900 and the newer 9989.

To our knowledge, no other microprocessor has been subjected to cosmic-ray-effects testing, but many bulk CMOS memories have been tested.

J. Memories

The memory area looks as if it will have more of a variety of types and vendors to choose from than the microprocessor area in the future. Efforts are going forward at Harris, RCA, Sandia Laboratories, Hughes, National Semiconductor, and TI to produce radiation-hardened memories.

Our main testing effort has centered on the RCA/Sandia-developed and Sandia-fabricated TCC-244, a 256 x 4 CMOS RAM similar to the CPD 1822D commercial RAM. Tests of the most recent devices[14] demonstrate functional capability after exposure to 1 Mrad. This RAM can be imprinted with a static data pattern if exposed to a substantial fraction of the failure dose with static data. On orbit, this would only occur if memory cells remained static for roughly a year at a time. We have seen this failure mode in our test results, but we believe it can be overcome by simple system considerations.

As a CMOS device, the TCC 244 should exhibit low susceptibility to cosmic rays[15,16] when operated at drain voltage V_{DD}=10 V. Sivo[17] predicts an upset rate of 2.7×10^{-10} per memory cell per day; this is felt to be conservative. RCA and Hughes plan to produce these hardened devices in the near future.

Harris Semiconductor has some interesting efforts going on in the static CMOS memory area as well. In a joint effort with Sandia, they are developing a 1K x 1 memory that is designed to be tolerant to 1 Mrad at V_{DD}=10 V. Harris is also working on a 6504 (4K x 1) RAM intended for 5-V operation and designed[18] to survive 500 krad. Its cosmic-ray susceptibility must be tested. We will evaluate these parts as soon as they become available. The only production I^2L memories actually tested (at Lincoln Laboratory) so far were Fairchild 93481's, of 1978 vintage. These failed at the unacceptable level of 20 krads, similar to the Fairchild 9440 microprocessor failure level.

TI is developing an I^2L memory (4K x 1) that will be TTL-compatible and is expected to have a radiation tolerance similar to the SBP 9900. This device will be faster and will require considerably more static power than CMOS, so it may be limited in its space applications. Its susceptibility to cosmic rays should be determined.

K. MSI and SSI Devices

RCA and National have produced many of the devices from the CMOS 4000-series logic family in rad-hard versions. These parts would support 10-V CMOS microprocessor systems. In some preliminary tests[19,20], they have functioned after exposure to 1 Mrad and are considered acceptable for flight with respect to radiation tolerance.

L. Cosmic-Ray Tests

On 26-27 May 1981, a variety of devices were tested for single-event upset from cosmic rays, including low-power TTL devices remaining from the LES-8/9 program (Bonded Stores) as well as some functionally identical devices constructed in different technologies[21] (e.g., LS-TTL, TTL, CMOS, and Schottky TTL). Basically, we were able to see bit-flips in each of the low-power TTL devices that we tested. The rates that we saw (10^{-1} flips per flip-flop cell per year) were higher than the observed rate on LES-8/9 ($\sim 3.8 \times 10^{-3}$). A prediction calculated by Binder, et al.,[22] of $\sim 10^{-2}$ falls between two observations. We believe that statistical error from the small sample size and the range of device response variability can account for the discrepancies between observation and theory. It should be noted, moreover, that since most devices appear to have an ionization threshold only marginally below that of the krypton ions use in the simulation, it is reasonable to assume that many of the cosmic rays in space fall short of depositing enough energy to cause a bit-flip. That is, the krypton simulation slightly overestimates the environment. Accounting for this would bring the orbital observations and simulation results into closer agreement.

Our tests showed a marked difference in susceptibility among various technologies. The LS-TTL devices tended to flip quite rapidly even at the weakest (0°) angle of incidence for energy deposition. Indeed, the LS-TTL devices showed nearly an order of magnitude higher bit-flip probability (at 1 per flip-flop per year) than their low-power TTL counterparts. On the other hand, TTL showed only a slight tendency to flip at the most severe (65°)

angle, and the one CMOS device we tested did not flip at all. The only Schottky device tested also had relatively low flip rates as compared to LS and low-power TTL.

One apparent conclusion from recent cosmic ray susceptibility tests is that CMOS parts are substantially harder to this threat when run at higher supply voltages.

M. Conclusions

In this section, the suitability of using currently available components in the natural environment of typical communication satellite orbits was assessed. After looking at the environmental threats in some detail, component hardness criteria of TID and BDEF for situations involving 1) no extra shielding and 2) a reasonable amount of extra shielding were established. Against these criteria, available hardware for on-orbit digital signal processing was examined. Two microprocessors, one RAM, and a family of MSI support chips were found which can meet the low-power consumption and radiation tolerance requirements of satellite applications. In addition, several developmental efforts were identified which show promise of additional useful memory components.

The research-scale efforts which have resulted in hardened components useful in the space environment are a necessary first step. They have produced encouraging results. However, this remarkable work is largely in vain if the parts cannot be produced reliably, reproducibly, and in sufficient quantity for future satellite programs. It is in the area of technology transfer to large-scale manufacturability that continued support is required.

V. TRAVELING WAVE TUBE AMPLIFIERS UPDATE

A. Introduction

The subject of traveling wave tube amplifiers, TWTAs, was addressed in exhaustive detail in previous reports.[1,2,3] The definition[3] of the TWTA and the basic principles of its operation were given. The currently active tube manufacturers of the free world were reviewed as to their capabilities and their known product-lines, and the global availability of TWTAs was assessed with special reference to EHF technology. The technological limits affecting these devices and the resultant producibility, availability, reliability, and cost issues were individually explored. The past performances, including operational experiences at all potential EHF MILSATCOM frequencies, were stated. Current research and development programs with their pertinent goals were described and recommended research and development efforts were given.

These, and other related issues, were treated in detail[3] both for the ground and for the space segments of present and future MILSATCOM systems and is incorporated herein by reference. The reader is urged to review this publication[3] in order to bring information presented here into better focus.

B. Follow-up

Manufacturers have made significant progress during the past eighteen months. The recent technological achievements in the areas of a) tubes, b) materials, c) circuits, d) manufacturing methods and technology, and e) thermionic engineering are discussed in the subsequent five sections.

1. Tubes

In this section, the recent technological accomplishments in the area of TWTAs is reviewed with special emphasis given to those programs mentioned in Reference 3. The present review does not include devices used in classified programs, powerful radar and electronic countermeasures tubes, fast-wave devices such as the novel peniotron and gyrotron -- even though these latter may have severe implications to communications as in jamming applications -- narrow band klystrons, extended interaction amplifiers, and other devices not directly used for communications purposes (e.g., high-power TWTAs at 95 GHz).

Rome Air Development Center (RADC) has sponsored two programs of specific interest to MILSATCOM system designers; one of them, the 60 GHz coupled-cavity TWT program at Hughes Aircraft Company, HAC, has delivered an acceptable engineering model TWTA. The amplifier was designed to have an output of 5 watts, and has achieved output level in excess of 7 watts. The other program sponsors Varian Associates in the development of an improved 8-year, 10 W, CW, PPM focused, helix TWTA operating between 40 and 44 GHz with 35 dB saturation gain, 35 dB noise figure, and at least 20% efficiency. This improved performance may be possible through the use of a diamond supported helical interaction structure which permits better thermal design and improved heat dissipation. At least one engineering model is expected at the end of the program in the Summer'81. A potential continuation of this program may result in a TWTA with 4 to 6 dB higher output power and a center frequency of 44.5 GHz. In connection with the development of this TWTA, the manufacturer developed a method of brazing diamonds to the helix and to the vacuum envelope

for good mechanical and thermal contact without carbonizing the diamond. Varian's success in this area represents a very important step in producing improved TWTAs.

Several EHF TWTA development programs are underway at Raytheon; they include:

1. The U.S. Air Force continues to sponsor V-band power TWT development at the Raytheon Company. The objective of this program is to develop a 500 W, CW, TWT with center frequency between 46 and 56 GHz, saturation gain of 40 dB, PPM focusing, and dc-to-rf conversion efficiency in excess of 15%.
2. Siemens is transferring their millimeter-wave tube manufacturing technology to Raytheon. A 38 GHz TWT currently being assembled at the Raytheon Microwave Power Tube Division Plant in Waltham, Massachusetts, represents the first product of this technology transfer effort.
3. Raytheon has delivered to the Air Force Wright Aeronautical Laboratories, Avionics Laboratory, the ASC-30 small EHF/SHF Airborne SATCOM System for the Air Force Satellite Communication System, AFSATCOM. The ASC-30 is a fifth generation microwave satellite communication terminal using a high output power TWTA operating at 40 GHz. The tube was built by Siemens; the high power amplifier module, including the high-voltage electronic power conditioners, was manufactured by Raytheon. The terminal will undergo operational evaluation in late 1981.

Hughes Aircraft Company under NASA-Lewis Research Center sponsorship is developing a dual-mode 21 GHz TWTA to operate with either 75 or 7.5 watts output power. This dual mode capability will permit added flexibility in the design of high priority MILSATCOM terminals. Evaluation of this tube during the latter half of '81 will determine its specific capability.

Watkins-Johnson Company, W-J, is currently developing a 25-50 W, PPM focussed, helix-type 21 GHz TWTA with a matching electronic power converter, EPC. The tube will be designed for a satellite-borne operation. Two tubes have been built, and initial test data is encouraging. A company goal to qualify the tubes for spaceborne use by the end of '81 is supported by internal research and development funds. The development of an EPC is proceeding in parallel with the tube development. The EPCs will be matched with the tubes to form a traveling wave tube amplifier transmitter.

The Ballistic Missile Defense Advanced Technology Center, BMDATC, of the U.S. Army sponsored the development, at Varian Associates, of a high-power broadband coupled-cavity, liquid-cooled, solenoid-focused TWTA for 35 GHz TWTA pulsed radar applications (Kwajalein Millimeter Radar). This tube is of interest to MILSATCOM system architects because it is designed to have a pulsed power output of 30 kW and 3 kW average. A development model has a peak power of 30 kW over 1 GHz bandwidth and an average power of 10 kW. The intended radar application is to amplify chirp waveforms where good phase and amplitude linearity are required. Development of this tube increases the technology base for MILSATCOM systems using time division multiple access.

A number of manufacturers, notably, Varian Associates, HAC, Raytheon, and Northrop, are developing helix TWTAs with an octave bandwdith (18 to 50 GHz) ~ 100 W average output power, ~ 40 dB gain, ~ 20% efficiency. Although the broad bandwidth may not be useful to MILSATCOM application, the design frequencies are appropriate. The effort has led one manufacturer to propose a 100 W, CW, 44 GHz, diamond supported helix TWTA for the Navy EHF Satellite Program, NESP. It is estimated that this tube will be available in the Summer of '83 and will cost ~ $15K per tube.

2. Materials

Programs for material development deal principally with cathode and electronic gun assembly constituents and manufacturing processes. A single important performance characteristic of the cathode is the density of the emitted current for a given operating life and the operating temperature. In general, as the temperature is increased, the emitted current density increases while the life decreases in an exponential manner. As operational frequencies increase and/or output power level increases, cathode emission density increase roughly in proportion. It is estimated that presently available cathodes satisfy emission density and life requirements for tubes operating < 20 GHz. These fundamental characteristics give rise to the current interest in materials research and life of cathodes, as discussed below.

Two programs, sponsored by the Air Force, at EMI-Varian, Ltd., and at the University of Dayton, deal with the physics and chemistry of thermionic emission by studying dispenser type cathodes and the nature of the emitting

surface and the transport of the active material from the matrix to the emitting surface, respectively. Both scanning electron microscope and Auger spectroscopic techniques are used in the experiments to locate the active emitting regions and to determine their properties. The latter program is directed toward more accurate and basic understanding of the emission mechanism. The goal of the program is to develop a model based on this understanding and to evaluate this model as to its usefulness in optimizing the cathode.

One new and promising technology is the controlled porosity cathode. Holes of microscopic dimensions are drilled with a laser into the tungsten, reportedly resulting in an "M-type" cathode with substantially more uniform emission over its surface than from cathodes in which the porosity is left to develop naturally. Field effect emission cathode developed at Stanford represents another technology under development and has been on life test at NASA-Lewis since mid'70s. Reportedly, up to 50 mA/mm^2 have been achieved, and there is potential emission densities up to 10 or perhaps 20 amperes per square centimeter. Life-tests on the M-type dispenser and B-type impregnated cathodes continue at NASA-Lewis Some 40,000 hours have been accumulated on the former and in excess of 50,000 hours on the latter, with current densities at the 2 and 4 A/cm^2. On the basis of current results and achievements with this type cathode, it is expected that a useful life of 11 years at (i.e., no significant diminishing electron emission) a current density of 1 A/cm^2 should be possible with an M-type cathode similar in design and material to those currently on life test.

A cathode life-test facilitiy being established at the Air Force Rome Air Development Center will permit current densities from 1 to 4 A/cm^2 and will allow for up to 40 life-test stations; each of which can test a device for at least 10 years. The first life tests are expected to begin by the end of 1981. In parallel with the establishment of this life-test facility, the Air Force is sponsoring the development of standard cathode life-test vehicles at Hughes Aircraft Company and Varian Associates. The program at HAC calls for the design, development, and delivery of twelve standard life-test "vehicles" to be used with a number of selected dispenser type cathodes of interest to both RADC and SAMSO. The program at Varian is for the development, fabrication, and delivery of thirty-six life-test vehicles. Each vehicle consists of an electron gun, ion blocking anode, PPM focussed drift space at ground potential, depressible collector, and a window for observing the emitting surface. Quality and purity of these materials in these test vehicles are required to be suitable for very long-term life-testing of the cathodes. Additionally, the Air Force is sponsoring, at Spectro-Mat, Inc., a cathode optimization study to improve reliability and the development of cold cathode field effect emission materials at Georgia Institute of Technology. The Air Force also is sponsoring a millimeter-wave cathode study program at HAC. The program effort will explore the properties of selected cathodes as they constrain the design of millimeter-wave tubes. After identifying the special requirements, if any, of mm-wave tubes, available cathodes will be matched with these requirements and evaluated experimentally.

The gun assembly of a TWTA may include, in addition to the cathode, other structures, e.g., grid(s), heater, and anode. Several Air Force-sponsored studies deal with the integrated design of the electron gun with primary emphasis on the effect that the grid, located in front of the cathode, has on the electron beam.

3. Circuits

A number of interaction circuit programs were discussed in Reference 3. Among these are the serpentine, or folded, waveguide, the comb-quad and tuneladder, and the ferruleless coupled cavity circuits. All these are for power levels in excess of those achievable with wire or tape wound helix interaction circuits, and all have affordable manufacturing costs of tubes as one of the prime goals. The folded waveguide interaction circuit is being developed at Raytheon with Air Force funding. It is expected that the first tube operating at approximately 44 GHz with ~ 0.5 kW output will be assembled and tested in the second half of 1981. If this development is successful, the manufacturing technology of the folded waveguide may result in a tube with performance comparable to a coupled-cavity design, but at a considerable reduction in the cost.

Ferruleless coupled-cavity circuit design reduces the costs of coupled-cavity TWTs, because those parts making up the interaction cavity can be stamped, instead of machined. Development of this type cavity is supported with Air Force and Navy funds. One tube has been built which has operational parameters (i.e., gain, bandwidth, and dc-to-rf conversion efficiency) comparable to those obtained with tubes made with conventionally machined cavities. Apparently the stamping technique produces parts that compare in

finish with machined parts, and at a significantly lower cost. Because a TWTA is both a labor and material intensive device, tubes made with ferruleless cavities are expected to cost less than conventional coupled-cavity tubes.

Wideband coupled-cavity circuit designs investigated at Varian Associates under Air Force sponsorship include tuneladder and comb-quad designs. It appears that the tuneladder theory is well understood, however, a tube using this design has not yet been built. Experimental evaluation of X-band tubes using the comb-quad circuit have substantiated theoretical expectations of gain, bandwidth, and power level. It is significant to note that the design features of this interaction circuit are applicable at K-band frequencies, and the manufacturing method seems to offer a significant cost savings.

Other circuit innovations involve the ubiquitous helix. In the twystron design study at Varian Associates, the broadband properties of the helix are combined with the power handling capability of klystrons. In the hightron investigations at Litton Industries, a helical waveguide replaces the many single cavities of a coupled-cavity design. It is hoped that this design also would combine the bandwidth capability of the helix with the power handling and thermal dissipation capability of the waveguide. The Air Force is sponsoring these programs and mm-wave helix technology at HAC and at Varian Associates. The common objectives of these programs is to establish improved helix type TWTA technology. These latter competing contracts have produced significant practical results in diamond supported helix, and in helix embedded in ceramic support material technologies. Both configurations show significantly improved thermal transfer properties indicating that an EHF helix TWTA with 100 W average power output may be possible by the mid 1980's.

4. Manufacturing Methods and Technology

Thermal dissipation capability of the helix interaction structure is much less than that of the coupled-cavity structures. Hence, TWTAs using the latter result in power generating capability which is orders of magnitude above that of a tube using a helix interaction structure. On the other hand, machining the 100 or so cavities required in a single coupled-cavity TWTA is a much more expensive process than manufacturing a helix with its supporting structure. The HAC Single Point Diamond Turned Millimeter Wave TWT Parts program, supported by the Navy addresses this problem. Development of diamond turning tools, holding fixtures, fabrication of coupled-cavities, and the evaluation of the rf performance of these parts in a coupled-cavity stack are the goals of the program. This precision machining technique uses a single diamond point as the cutting tool of a computer-controlled lathe in a temperature controlled environment. The machining tolerances achievable are about 10 microinches, and the resultant finish after a single pass of the diamond tipped tool is described as mirror-like. The machining cost of the finished coupled-cavity is five to ten times less than parts produced by customary machining methods. Because of the improved precision of the parts, the structure is more easily assembled, requires less adjustment, and there are few rejected parts.

C. Thermionic Engineering

Engineering training in the tube technology is on the verge of extinction in the U.S.A. The problem and its criticality has been recognized for some time, and a program is in existence since 1976 to reinstate graduate training

in microwave tube engineering in order to prevent the foreseeable shortage of qualifed tube engineers. There is a sponsored two-year graduate curriculum at Stanford University with the cooperation of the seven major tube companies. The annual budget of nearly one million is shared on a basis of thirty percent each from the Army, Navy, and Air Force, and ten percent from NASA. The first class began with eight students in September 1977, six of these graduated, but only five of the starting eight are practicing tube design. Subsequent classes had similar or lower yield; the full quota of 12 students in one class has not been achieved. The program appears to have difficulties in attracting and in keeping students. This is a vital program with important objectives impacting on the defense of the country, and it appears to be faltering.

D. The $1,500 TWT

1. Overview

In spite of the intrinsically high price of TWTAs, their usefulness for satellite communications systems is well established both in space and ground terminals applications. Four unique characteristics of TWTs are:

a. amplification with high-gain

b. broad bandwidth

c. large output power

d. good dc-to-rf conversion efficiency.

The TWT is an attractive alternative for the power amplifier in MILSATCOM terminals especially if these unique characteristics were available for an affordable price.

Recently a search for low cost TWTs was carried out to determine that, if such devices exist, what makes them inexpensive, and whether the technology that resulted in the low cost per tube is applicable to the power amplifier requirements of MILSATCOM terminals. As a result, a specific affordable TWTA with appropriate performance characteristics was found; the tube reportedly costs ~ $1,500 each when procured in quantities of 10,000 or more. The performance characteristics of the TWT, the application, the operational experience, and the contributing factors that helped to reduce the price to $1,500 per tube are described in this section. There are no known production lines for EHF TWTAs, but there are several sponsored developments. One of these described below may produce TWTAs which satisfy EHF MILSATCOM terminal applications. Development of this capability depends on advances in h lix technology. If these advances occur, and if the mass-production techniques successful with devices operating below 20 GHz can be applied to work at 45 GHz, a TWTA for an EHF MILSATCOM terminal may cost ~ $5,000 per tube in quantities of 1,000. The estimated cost of the associated high voltage power supply is $2,000 each.

2. The $1,500 TWT

The AN/SLQ-32 ESM/EW suite for shipborne ASMD (Electronic Support Measures/Electronic Warfare, Anti-Ship Missile Defense) system has a transmitter set which requires 140 TWTAs that have a matched transfer function over more than an octave frequency range and a 3-dB range of input power. The tubes operate over the I-J frequency bands, produce 40 W of average power each, and clusters of 18 tubes are powered from a single dc high voltage

source. The operational experience indicates ~ 10,000 hours MTBF and about 5% of the transmitters fail. Less than half of these failures, or about 2%, are due to the TWT. The cost of the individual tubes is ~ $1,500. One manufacturer is Varian Associates; other potential suppliers are Raytheon and ITT.

The principal contributing factor for the low price is that the order for 10,000 tubes is probably the largest single order for TWTs ever made. A manufacturing technology program and other cost reducing practices -- e.g., reducing parts count, automating assembly and testing, subassembly fabrication in large, repetitive cycles, early elimination of defective materials, and virtually no adjustments -- helped to lower manufacturing costs by 55% since completion of the 500^{th} unit.

3. Applicability to MILSATCOM

Several manufacturers and others were contacted for the purpose of exploring the implications of large volume production of EHF TWTs for MILSATCOM terminals. Varian Associates is currently sponsored by Rome Air Development Center to design, fabricate, evaluate, qualify, and deliver a 10 W CW helix TWTA. The tube will operate from 40 to 44 GHz, have 35 dB gain, 35 dB noise figure, greater than 20% efficiency, and a useful life in excess of 70,000 hours. The project started in 1979, and it is about to be completed. Assuming they meet their objectives and are given a follow-up order for 1000 more identical TWTs, Varian Associates estimates that the tubes will cost $5,000 each.

REFERENCES

1. D. J. Frediani et al., "Technology Assessment for Future EHF MILSATCOM Systems," ICC '81 Record II, Denver, 14-18 June 1981, pp. 36.2.1-36.2.7.

2. D. J. Frediani, "Technology Assessment for Future MILSATCOM Systems: The EHF Bands," Project Report DCA-5, Lincoln Laboratory, M.I.T. (12 April 1979) , DDC AD-A071886.

3. D. J. Frediani, M. L. Stevens, and S. Zolnay, "Technology Assessment for Future MILSATCOM Systems: An Update of the EHF Bands," Project Report DCA-7, Lincoln Laboratory, M.I.T. (1 October 1980), DTIC AD-B053555.

4. S. D. Personik, Optical Fiber Transmission Systems (Plenum Press, New York, 1980).

5. J. M. Wozencraft and I. M. Jacob, Principles of Communication Engineering (Wiley, New York, 1968).

6. R. C. Williamson, "Comparison of Surface Acoustic-Wave And Optical Signal Processing," Proc. SPIE Vol. 185: Optical Processing System (Society of Photo-Optical Instrumentation Engineers, Bellingham, Washington, 1979), pp. 74-84, DDC AD-A076429/0.

7. N. Wilkin, C. T. Self, and H. Eisen, "Ionizing Dose Rate Effects in Microprocessors," IEEE Trans. Nucl. Sci. NS-27, 1420, (1980).

8. E. E. King and R. L. Martin, "Effects of Total Dose Ionizing Radiation on the 1802 Microprocessor," IEEE Trans. Nucl. Sci. NS-24, 2172 (1977).

9. G. J. Brucker, P. Measel, and K. Wahlin, "Transient Radiation Responses of Hardened CMOS/SOS Microprocessor and Memory Devices," IEEE Trans. Nucl. Sci. NS-27, 1432 (1980).

10. F. G. Walther, "Radiation Test of Fairchild 9440 Microprocessor," private communication.

11. H. J. Ouellet, "Summary of Radiation Tests Performed on Seven Mil. Spec. SBP 9900 ANJ Microprocessors Tested August 1980," private communication.

12. T. Ellis, "Radiation Effects Characterization of the SBP 9900, A 16-bit Microprocessor," IEEE Trans. Nuc. Sci. NS-26, 4735 (1979).

13. W. E. Price, Jet Propulsion Laboratory, Pasadena, CA, private communication.

REFERENCES (cont'd)

14. J. P. Woods, "Latest TCC 244 RAM Radiation Hardness Test Description and Results," private communication.

15. W. A. Kolasinki, et al., "Simulation of Cosmic-Ray Induced Soft Errors and Latchup in Integrated-Circuit Computer Memories," IEEE Trans. Nucl. Sci. NS-26, 5087 (1979).

16. C. S. Guenzer, et al., "Single Event Upsets in RAMs Induced by Protons at 4.2 GeV and Protons and Neutrons Below 100 MeV," IEEE Trans. Nucl. Sci. NS-27, 5042 (1980).

17. L. L. Sivo, et al., "Cosmic Ray-Induced Soft Errors in Static CMOS Memory Cells," IEEE Trans. Nucl. Sci. NS-26, 5042 (1979).

18. F. G. Walther, "Radiation Tolerant Memory Developments," private communication.

19. J. K. Roberge, "Radiation Tests of the RCA 4066 Analog Switch," private communication.

20. J. P. Woods, "Radiation Hardness Tests on RCA 4001 and 4007 and National 4601 Devices," private communication.

21. J. P. Woods, et al., "Investigation for Single Event Upset in MSI Devices," IEEE Trans. on Nuclear Science (to be published in NS-28, 1981).

22. D. Binder, et al., "Satellite Anomalies from Galactic Cosmic Rays," IEEE Trans. Nucl. Sci. NS-22, 2675 (1975).

UNCLASSIFIED

SECURITY CLASSIFICATION OF THIS PAGE (When Data Entered)

REPORT DOCUMENTATION PAGE		READ INSTRUCTIONS BEFORE COMPLETING FORM
1. REPORT NUMBER ESD-TR-81-333	2. GOVT ACCESSION NO. AD-A112503	3. RECIPIENT'S CATALOG NUMBER
4. TITLE (and Subtitle) Technology Assessment: Optical Communications, Signal Processors, and Radiation Effects		5. TYPE OF REPORT & PERIOD COVERED Project Report 6. PERFORMING ORG. REPORT NUMBER Project Report DCA-11
7. AUTHOR(s) Leon J. Ricardi, Don M. Boroson, Vincent W.S. Chan, B.H. Hutchinson, Frederick G. Walther, John P. Woods, and Stephen L. Zolnay		8. CONTRACT OR GRANT NUMBER(s) F19628-80-C-0002
9. PERFORMING ORGANIZATION NAME AND ADDRESS Lincoln Laboratory, M.I.T. P.O. Box 73 Lexington, MA 02173		10. PROGRAM ELEMENT, PROJECT, TASK AREA & WORK UNIT NUMBERS Program Element Nos. 63431F, 33601F and 33126K Project Nos. 2029 and 6430
11. CONTROLLING OFFICE NAME AND ADDRESS Air Force Systems Command, USAF Andrews AFB Washington, DC 20331 Defense Communications Agency 8th Street & So. Courthouse Square Arlington, VA 22204		12. REPORT DATE 7 January 1982 13. NUMBER OF PAGES 96
14. MONITORING AGENCY NAME & ADDRESS (if different from Controlling Office) Electronic Systems Division Hanscom AFB, MA 01731		15. SECURITY CLASS (of this report) Unclassified 15a. DECLASSIFICATION DOWNGRADING SCHEDULE

16. DISTRIBUTION STATEMENT (of this Report)

Approved for public release; distribution unlimited.

17. DISTRIBUTION STATEMENT (of the abstract entered in Block 20, if different from Report)

18. SUPPLEMENTARY NOTES

None

19. KEY WORDS (Continue on reverse side if necessary and identify by block number)

technology survey
LASERCOM
radiation hazard
on-board signal processor
SAW demodulator
traveling wave tube

20. ABSTRACT (Continue on reverse side if necessary and identify by block number)

Military satellite communication system architects are often constrained by the performance capability of technology limited devices. Consequently, it is important to continually assess that technology essential to the support of future MILSATCOM systems. This project report and those published previously[1,2,3] summarize study efforts that developed strawman MILSATCOM systems which satisfy projected user requirements. The technology requisite to deployment of these SATCOM systems was carefully evaluated, and required improvements were described and/or defined. Previously[1,2,3], the study was limited to rf devices or related phenomena. This report considers optical communication systems, on-board signal demodulators, and radiation effects. An update on the traveling-wave tube technology is presented because of its extreme importance to the development of affordable MILSATCOM terminals.

DD FORM 1 JAN 73 1473 EDITION OF 1 NOV 65 IS OBSOLETE

UNCLASSIFIED

SECURITY CLASSIFICATION OF THIS PAGE (When Data Entered)


04